Integrin alpha 1 beta 1 has limited influence on epidermal growth factor receptor signaling but sex-dependent effects on estrogen receptor beta in murine knee chondrocytes

by

Alicia Black

A Thesis

presented to

The University of Guelph

In partial fulfilment of requirements
for the degree of

Masters of Science

in

Human Health & Nutritional Sciences

Guelph, Ontario, Canada

ABSTRACT

INTEGRIN ALPHA 1 BETA 1 HAS LIMITED INFLUENCE ON EPIDERMAL GROWTH FACTOR RECEPTOR SIGNALING BUT SEX-DEPENDENT EFFECTS ON ESTROGEN RECEPTOR BETA IN MURINE KNEE CHONDROCYTES

Alicia Black Advisor: Dr. Andrea Clark
University of Guelph, 2020

Integrin α1β1 protects against OA development when it is upregulated in the early stages of disease development. One possible mechanism through which integrin α1β1 affords this protection is through suppression of growth factor receptor signaling pathways, including EGFR. The interplay of integrin α1β1 and EGFR in post-traumatic OA is sex-dependent, suggesting ERs may also participate. The purpose of this thesis was to evaluate the percent of knee chondrocytes immunostained for pEGFR, 3-nitrotyrosine, ERα and ERβ in *itga1*-null and wild type mice. We show that integrin α1β1 had limited influence on the percent of chondrocytes stained positively for pEGFR or 3-nitrotyrosine. In contrast, we found that integrin α1β1 did influence ERα and β expression that were co-expressed as well as co-localized in chondrocytes. Understanding the molecular mechanisms underlying the development of OA is essential for the development of effective, individualized, sex-specific treatments in this age of personalized medicine.

ACKNOWLEDGEMENTS

This work was funded by a Canadian Institutes of Health Research Open Operating Grant (AC).

I would like to first thank my family and friends, especially my parents, Alex and Lucie Black, for their endless love, support, and encouragement throughout my life.

To my advisory committee, Dr. Thomas Koch and Dr. John Srbely, thank you for your encouragement and guidance through my research project.

I would like to thank Valerie Wai and Jana Michaud for lending their wisdom, technical experience, and immense generosity and support throughout my MSc journey. Thank you for being so welcoming and such amazing friends.

Thank you to Victoria Lawson and Sienna Cole for their diligent work on the analysis of all the experiments throughout my research project.

Also, I would like to acknowledge Elizaveta Shpilevaia for volunteering so much of her time to dissect, embed, and cut beautiful sections to use in my experiments.

To the other members of the Clark lab, and the friends I've made in the HHNS department, thank you for making my last few years at Guelph some of the best.

Thank you to Michaela Strüder-Kypke for providing technical support and assisting with the confocal microscope.

Thank you to Nada Hafez for lending her expertise and providing assistance on the statistical analysis of my experiments.

Last but certainly not least, Dr. Andrea Clark, I want to thank you for taking a chance and being patient with me as my advisor. You taught me not only about the world of animal research, histology and confocal microscopy, but also how to be an effective and zealous supervisor and researcher.

TABLE OF CONTENTS

LIST OF FIGURES

LIST OF SYMBOLS, ABBREVIATIONS OR NOMENCLATURE

α	Alpha (greek letter)
ABC	Avidin-biotin complex
ADAMTS5	A disintegrin and metalloproteinase with thrombospondin motifs 5
Akt	Protein kinase B
ANOVA	Analysis of variance
β	Beta (Greek letter)
$[Ca^{2+}]_i$	Calcium cation
DMM	Destabilization of the medial meniscus
DNA	Deoxyribonucleic acid
EGF/*Egfr*	Epidermal growth factor (protein)/(gene)
EGFR	Epidermal growth factor receptor
ERα	Estrogen receptor alpha
ERβ	Estrogen receptor beta
ErbB	Receptor family of tyrosine kinases
ERK	Extracellular signal-regulated kinase
HB-EGF	Heparin-binding epidermal growth factor-like growth factor
H_2O_2	Hydrogen peroxide
HPMC	Hydroxypropyl methylcellulose
Itga1	Integrin α1-encoding gene
Itga2	Integrin α2-encoding gene
JAK	Janus kinase
MAPK	Mitogen-activated protein kinase

MicroCT	Micro computed tomography
MIG-6/*Mig6*	Mitogen-inducible gene 6 (protein)/(gene)
MMP13	Matrix metalloproteinase 13
mRNA	Messenger ribonucleic acid
NADPH	Nicotinamide diadenine nucleotide phosphate
NO	Nitric oxide
NOX	NADPH oxidase
$\cdot O_2^-$	Superoxide
OA	Osteoarthritis
OH^-	Hydroxyl anion
$ONOO^-$	Peroxynitrite
PBS	Phosphate buffer saline
P13K	Phosphatidylinositol 3-kinase
pEGFR	Phosphorylated epidermal growth factor receptor
PKC	Protein kinase C
PLCg	Phospholipase Cg
ROS	Reactive oxygen species
SMAD	Substrates for TBR kinases
Src	Non-receptor tyrosine kinase
STAT	Signal transducers and activators of transcription
TBR	Transforming growth factor receptor
TGFα	Transforming growth factor alpha
TGFβ	Transforming growth factor beta

μm	Micron
μL	Microlitre

LIST OF APPENDICES

1 Introduction

1.1 Cartilage and Chondrocytes

Cartilage is a highly specialized tissue designed to provide a smooth, lubricated surface to facilitate joint articulation and movement (Fox *et al.* 2009). Based on molecular composition, there are three main types of cartilage present throughout the body: hyaline, elastic, and fibrocartilage (Umlauf *et al.* 2010). Hyaline cartilage is of particular interest to this thesis. It is predominantly associated with the skeletal system and includes articular cartilage (Umlauf *et al.* 2010). Articular cartilage lacks blood vessels, nerves, and lymphatics and thus, has a limited capacity for repair and regeneration (Fox *et al.* 2009). Water makes up to 80% of the wet weight of articular cartilage and it is the molecular interactions of water with extracellular matrix components that influences the unique mechanical properties of the tissue (Buckwalter and Mankin 1997). This extracellular matrix consists of proteoglycans such as aggrecan, collagens (types II, VI, IX, X, and XI), and other glycoproteins including anchorin, cartilage oligomeric protein, fibronectin and tenascin that are present in smaller amounts (Buckwalter and Mankin 1997). Chondrocytes are the exclusive, largely isolated cells residing in articular cartilage that are distributed throughout the extracellular matrix making up about 2% of total cartilage volume (Fox *et al*. 2009).

Articular cartilage can be divided into four zones characterized by distinct cellular organization: the superficial, middle and deep zones, as well as the calcified cartilage zone which interfaces with the subchondral bone (Wong and Carter 2003). The superficial zone contains chondrocytes that are more elliptical in shape with their long axis parallel to the articular surface and collagen fibers that are similarly aligned (Fox *et al.* 2009; Lees and Partington 2016). This is

the zone that is in direct contact with the synovial fluid and that protects the deeper zones from shear stresses (Fox *et al.* 2009). This defense is largely achieved by the glycoprotein lubricin, also known as proteoglycan 4, which is highly expressed by superficial zone chondrocytes as well as synoviocytes (Rhee *et al.* 2005). The middle zone comprises 40-60% of the total cartilage volume and contains large proteoglycan aggregates and thicker collagen fibers which are obliquely arranged (Fox *et al.* 2009; Lees and Partington 2016). There are less chondrocytes in this zone and they are more spherical in shape (Fox *et al.* 2009; Lees and Partington 2016). The deep zone has collagen fibers that are arranged perpendicular to the articular surface, the highest proteoglycan content, and chondrocytes that are commonly arranged in columns running parallel to the collagen fibers (Fox *et al.* 2009; Lees and Partington 2016). Together, the proteoglycan rich middle and deep zones are crucial in the defense against compressive forces (Fox *et al.* 2009; Lees and Partington 2016). The negative charges associated with the proteoglycan molecules repel one another and hold water molecules in the extracellular matrix, working together to resist compression of the cartilage (Maroudas *et al.* 1980). Separating the deep zone from the calcified cartilage zone is the tide mark which is a cell-free layer found only in joint cartilage (Fox *et al.* 2009; Lees and Partington 2016). The calcified cartilage zone is critical for holding the cartilage to the bone via anchoring of the deep zone collagen fibers to the subchondral bone (Fox *et al.* 2009). There are fewer chondrocytes in this layer and they are hypertrophic, at the end stage of differentiation (Fox *et al.* 2009; Lees and Partington 2016).

Within articular cartilage, collagens II, VI, IX, X, and XI are all found in the extracellular matrix with collagen II being the most abundant and collagen VI primarily localized around the chondrocytes in the pericellular matrix (Buckwalter and Mankin 1997; Goldring 2012). The

pericellular matrix is a 1-5 μm region directly surrounding the chondrocytes, adjacent to the cell membrane (Fox *et al.* 2009; Vincent 2013). This region plays a critical role in the initiation of signal transduction within the chondrocytes in response to mechanical stress through interaction with cell surface receptors such as integrins (Fox *et al.* 2009; Vincent 2013). Further contributing to the unique mechanical properties of cartilage is the distinct organization of the collagen fibril network throughout the different zones. As described above, collagen fibers run perpendicular to the calcified cartilage in the deep zone, arch and intersect with each other in the middle zone (as originally described by Benninghoff in 1925), and then run parallel with the articular surface in the superficial zone (Kaab *et al.* 1998). Collagen fibres provide cartilage with tensile strength, resisting deformation of the superficial zone and facilitating the transmission of loads from the surface to the middle and deep zones (Kaab *et al.* 1998).

An additional component of the extracellular matrix are proteoglycans such as aggrecan. These molecules consist of a protein core and one or more glycosaminoglycan chains extending perpendicularly and forming brush-like projections which carry a negative charge (Maroudas *et al.* 1980; Ratcliffe *et al.* 1984; Buckwalter and Mankin 1997). Common glycosaminoglycans found in articular cartilage include chondroitin sulfate, keratan sulfate, and dermatan sulfate (Buckwalter and Mankin 1997). These molecules can aggregate through binding to hyaluronic acid (Ratcliffe *et al.* 1984). The formation of aggregates anchors proteoglycans within the extracellular matrix, ensuring they remain in place during tissue deformation and maintaining the integrity of the proteoglycan and collagen meshwork (Buckwalter and Mankin 1997). Osmotic pressure is created by these hydrophilic proteoglycans within the cartilage due to the presence of these negatively charged groups that draw water into the tissue (Maroudas *et al.* 1980; Lees and

Partington 2016). Therefore, the gradient of increasing glycosaminoglycan content from the articular surface through the middle zone to the deep zone creates a gradient of osmotic pressure in the tissue and thereby decreases the tension on the local collagen network (Maroudas *et al.* 1980). Due to this osmotic draw, proteoglycans and associated molecules give cartilage strength under compression (Maroudas *et al.* 1980).

1.1.1 Osteoarthritis

Degenerative conditions such as osteoarthritis (OA) often disrupt the intricate organization of articular cartilage. OA is a regressive joint disease which is characterized by articular cartilage deterioration, breakdown of the extracellular matrix, and ultimately, joint remodeling (Umlauf *et al.* 2010). The first degenerative changes in articular cartilage are commonly fibrillation, characterized by softening of the articular cartilage and development of lesions or splits (Poole 1999). Other hallmark signs of the OA phenotype include chondrocyte proliferation and associated increase in matrix synthesis, loss of proteoglycan and glycosaminoglycan content, osteophyte formation, and synovitis (Maroudas and Venn 1977; Umlauf *et al.* 2010). Ultimately for the patient, this manifests as inflammation, joint pain and stiffness and subsequent reduced mobility and quality of life. As such, OA is a leading cause of disability in North American affecting about 1 in 6 adults (Arden *et al.* 2008; Glyn-Jones *et al.* 2015). In fact, the total direct cost of OA in Canada is estimated to be about $2.9 billion and expected to increase 2.6-fold by 2031 (Sharif *et al.* 2015). Although much of the focus is on the direct healthcare costs associated with OA, there are also noteworthy indirect medical costs (for example having to take time off work, not being able to perform household chores, etc.), therefore, the true economic impact of OA is often underestimated (Gupta *et al.* 2005). Together,

this demonstrates the tremendous burden on individuals living with OA as well as on the national healthcare system.

Many risk factors have been associated with OA including, obesity, age, sex, and joint trauma, though the exact cause of OA pathogenesis remains unknown. Older adults are primarily affected by OA with about 27% of individuals below the age of 70 receiving the diagnosis compared to 44% over the age of 80 (Felson *et al.* 1987). Additionally, obesity is associated with the incidence of OA in both weight-bearing and non-weight-bearing joints, with studies reporting a seven-fold increased risk of developing OA for obese patients (BMI > 30 kg/m$_2$) (King *et al.* 2013). Finally, while the prevalence of OA is similar between males and females until around the age of 50, later in life females are twice as likely to develop OA compared to males (Arden and Nevitt 2006; Ding *et al.* 2006). This is true of hand and knee OA, as well as hip OA to a lesser extent (Arden and Nevitt 2006; Ding *et al.* 2006). Of critical importance to the study of the degenerative changes in OA is the anatomical organization of the joints affected, with the knee being of particular interest to this thesis.

1.2 Knee Loading

While OA can affect many joints of the body including the knee, hip, hand, foot, ankle and spine, the knee is one of the most common. As a weight-bearing hinge joint, the knee is comprised of bones, ligaments, menisci and cartilage encapsulated in a synovial membrane which functions in the transmission of biomechanical loads in the lower limb (Eckhoff 2005; Abulhasan and Grey 2017). The knee includes the articulation of the femur and tibia, as well as the femur and patella, all with cartilage on the articular surfaces to provide a smooth, lubricated interface for efficient joint movement (Fox *et al.* 2009; Abulhasan and Grey 2017). The distal

femur has a distinct asymmetrical shape with two rounded condyles that articulate with the flattened tibial plateaus on the proximal end of the tibia (Eckhoff 2005; Shenoy *et al.* 2013). Of the two condyles, the medial condyle has the larger area of articulation allowing for anterior translation and external rotation of the tibia during knee extension and the lateral condyle has the larger radius which causes internal rotation during flexion (Shenoy *et al.* 2013). Furthermore, the medial femoral condyle and medial tibial plateau are more elongated than their lateral counterparts (Flandry and Hommel 2011). This coronal asymmetry of the articular surfaces of the knee contributes to increased loading in the medial compared to the lateral compartment of the knee (Flandry and Hommel 2011; Shenoy *et al.* 2013) and results in the screw-home mechanism, or internal rotation, that occurs during the terminal extension of the knee during standing (Flandry and Hommel 2011; Shenoy *et al.* 2013).

In addition to differences in the shape of the articular surfaces of the femur and tibia, the wear on the articular cartilage of these bones is also influenced by the frequency and duration of the loading they experience. Opposing articular surfaces experience equal contact forces, however the duration of the load experienced by the articular cartilage can be quite different (Clark *et al.* 2005; Clark 2008). For example, one would expect the tibial plateaus and patellar surface to be more consistently loaded compared to the intermittent loading experienced on the femoral condyles and groove throughout the range of motion of the knee. Intermittent loading of the joint allows synovial fluid to provide continuous nourishment whilst also getting rid of waste, however this effect is diminished in static loading (Clark 2008). Thus, it is perhaps not surprising that more cartilage damage is seen on the statically loaded surfaces, such as the tibial plateaus and patellar surface.

Further influencing the distribution of forces as well as stabilization of the knee are the menisci and ligaments. The medial and lateral menisci are located between the tibiofemoral articulations and are crescent-shaped wedges of fibrocartilage that increase the surface area for load transmission and absorb shock during dynamic motion (Fox *et al.* 2012; Abulhasan and Grey 2017). The menisci differ in shape with the medial meniscus being broader but with a thinner body than the lateral meniscus, though both have concave superior surfaces, allowing for smooth articulation with the convex femoral condyles (Fox *et al.* 2012; Flandry and Hommel 2011). Also acting to stabilize the knee are ligaments, including the medial and lateral collateral ligaments, and the anterior and posterior cruciate ligaments (Flandry and Hommel 2011; Abulhasan and Grey 2017). The medial collateral ligament restrains valgus stress and aids in controlling tibial rotation (Miller 2009). It originates on the superomedial aspect of the medial femoral condyle and inserts on the medial aspect of the proximal tibial shaft (Miller 2009). The lateral collateral ligament is the primary restraint against varus opening of the knee (Bowman and Sekiya 2009). It originates on the superolateral aspect of the lateral femoral condyle between the insertion of the popliteus tendon and the lateral gastrocnemius and inserts distally on the fibula (Bowman and Sekiya 2009; Miller 2009). The anterior cruciate ligament (ACL) originates on the posterolateral surface of the intercondylar notch and travels anteriorly to insert on the intercondylar eminence (Flandry and Hommel 2011). It functions primarily to resist anterior translation of the tibia relative to the femur (Flandry and Hommel 2011). Additionally, the ACL guides the tibial rotation during the screw-home mechanism of knee extension (Flandry and Hommel 2011). In contrast, the posterior cruciate ligament originates on the medial surface of the intercondylar notch and inserts on the posterior aspect of the proximal tibia and functions primarily to resist posterior translation of the tibia relative to the femur (Flandry and Hommel

2011). Together, the menisci and the cruciate ligaments function to stabilize the joint and guide the femoral condyles over the surface of the tibial plateaus during knee flexion and extension (Eckhoff 2005; Abulhasan and Grey 2017). These structures are commonly affected in joint injury, destabilizing the joint and altering the transmission of loads in the knee, thereby putting strain on the articular cartilage and leading to the initiation and progression of degenerative conditions such as OA (Andriacchi 1994).

In addition to ligament or meniscal injury, knee alignment (the hip-knee-ankle angle) can influence load distribution at the knee (Sharma *et al.* 2001; Shenoy *et al.* 2013). Varus alignment is described as "bowed knees," where the tibia is rotated somewhat medially in relation to the femur resulting in an outward turned knee, whereas valgus alignment is referred to as "knocked knees," where the tibia is rotated laterally in relation to the femur resulting in an inwardly rotated knee (Brouwer *et al.* 2007; Sharma *et al.* 2010; Kumar *et al.* 2015). Kumar *et al.* (2015) assessed the association of varus/valgus alignment with OA development by measuring differences between males and females in cartilage composition and walking mechanics in healthy and OA populations. In agreement with others, they found that varus alignment is associated with an increased risk of medial knee OA while valgus alignment is associated with lateral knee OA (Sharma *et al.* 2013; Kumar *et al.* 2015). Therefore, gross biomechanical variances such as joint malalignment have been identified as contributing to altered load distribution across joints and thus increased risk of OA development.

1.2.1 Chondrocyte Response to Compression

Understanding the biomechanical response of chondrocytes to compression provides insight into mechanical triggers of intracellular signaling that might lead to degenerative changes

in cartilage. Comparison of cartilage from the medial femoral condyle of rabbits in weight-bearing (posterior) versus less-weight-bearing (anterior) regions showed that the more loaded area had thicker cartilage, an overall increase in cell volume and density, and fewer chondrocytes present in the superficial zone compared to unloaded regions (Eggli *et al.* 1988). In a similar manner, cartilage from the more consistently loaded feline patella is twice as thick, and the chondrocytes near the surface more rounded in shape and the deep zone columns of cells more numerous compared with the intermittently loaded femoral groove (Clark *et al.* 2003). Furthermore, under the same load, the patellar cartilage experiences more strain than the femoral groove cartilage and the chondrocytes in the top 40% of patellar cartilage depth undergo greater deformation compared to their femoral counterparts (Clark *et al.* 2003). Importantly, changes in chondrocyte shape via mechanical deformation have been identified as a possible regulator of cartilage metabolic activity (Broom and Myers 1980). Furthermore, in articular cartilage explants, cyclic compression is known to stimulate proteoglycan and matrix synthesis (Sah *et al.* 1989), while static compression suppresses it (Jones *et al.* 1982). Static loading has also been shown to limit the rate of transport of macromolecules such as growth factors, hormones, enzymes and cytokines to chondrocytes (O'Hara et al. 1990), as well as altering local ion concentrations and nuclear shape (Kim *et al.* 1994; Freeman *et al.* 1994). Taken together, these data support the idea that chondrocytes located in different regions of cartilage experience different magnitudes and rates of loading, thereby contributing to contrasting metabolic activity. Thus, the chondrocyte/extracellular matrix interface mediated by receptors such as NG2, annexin V, CD44 and integrins (McGlashan *et al.* 2006) is critical in influencing the metabolic activity of chondrocytes and thus the health of articular cartilage.

1.3 Integrins

Integrins are transmembrane collagen receptors expressed by chondrocytes. They participate in outside-in (altering gene expression) and inside-out (altering expression and affinity of receptors) signaling in response to mechanical load on cartilage (Loeser *et al.* 2000). Integrins are heterodimeric, composed of an α and β subunit that have both extracellular domains binding to matrix components, and cytoplasmic domains involved in the activation of various intracellular signaling cascades (Hynes 2002; Tian *et al.* 2015). There are 24 possible integrin heterodimers made from a combination of one of eight β subunits and one of 18 α subunits (Hynes 2002). Chondrocytes express various isoforms including α1-6, as well as β1, 3 and 5 (Salter *et al.* 1992; Loeser *et al.* 2000; Tian *et al.* 2015). Of particular interest to this thesis is integrin α1β1. Integrin α1β1 is an important extracellular matrix receptor for chondrocytes, binding collagens type II and VI (Loeser *et al.* 1995; Loeser 1997) and is upregulated in both the pre-clinical stages of OA, before cartilage degradation begins, and end stage OA (Loeser *et al.* 1995; Zemmyo *et al.* 2003). Integrin α1β1 includes the α1 subunit that binds exclusively to the β1 subunit, and thus deletion of the α1 subunit in mice (*itga1*-null) renders them deficient in integrin α1β1, while leaving the other partnerships of the β1 subunit untouched (Gardener *et al.* 1996). Importantly, studies utilizing *itga1*-null mice have demonstrated that integrin α1β1 plays a protective role against both spontaneous and post-traumatic OA.

Itga1-null mice develop spontaneous OA about two to three months earlier compared to wild type mice, though sex differences were not considered (Zemmyo *et al.* 2003). Additionally, Shin *et al.* (2016) performed surgery to destabilize the medial meniscus of *itga1*-null and wild type mice and assessed the onset and progression of post-traumatic OA in the knee using

microCT and histological approaches. They found a sex-dependent (female only) protective effect of integrin α1β1 with *itga1*-null mice showing signs of cartilage degeneration one month earlier than wild type controls (Shin *et al.* 2016). Together these data suggest that integrin α1β1 protects against both spontaneous and post-traumatic OA when it is upregulated in the early stages of disease, however this protection is more robust in females compared to males. The molecular mechanisms underlying this chondroprotective effect are not yet well understood.

One emerging theory for the mechanism through which integrin α1β1 protects against OA is through the interplay of integrin α1β1 and growth factor receptor signalling pathways, including transforming growth factor β receptor II (TBRII) and epidermal growth factor receptor (EGFR). Integrin α1β1 is known to downregulate the activity of these receptors through a common mechanism involving T-cell protein tyrosine phosphatase, thereby facilitating the balance between anabolic and catabolic processes within cartilage (Chen *et al.* 2007).

1.4 Growth Factor Receptors

TBRII is activated by transforming growth factor β (TGFβ), one of the most potent stimulators of fibrosis (Parekh *et al.* 2011). Activation of TBRII leads to the serine phosphorylation and activation of TBRI, initiating the SMAD-dependent pro-fibrotic cascade, tight regulation of which should protect against cartilage degradation (Chen *et al.* 2014). While TGFβ signaling is largely considered protective against the initiation and progression of OA (Pujol *et al.* 2008), it has been shown that mice having large amounts of TGF-β1 in the knee can result in OA in the mouse. Specifically, multiple injections of high dose TGFβ-1 into murine knee joint resulted in cartilage damage and formation of osteophytes consistent with results of experimental OA models (van Beuningen *et al.* 1994; van Beuningen *et al.* 2000). Additionally,

overexpression of active TGFβ-1 in murine knee joints resulted in OA-like changes including synovial hyperplasia and osteophyte formation (Bakker *et al.* 2001). Together, these studies suggest that heightened TBR activity could result in excessive fibrotic activity in the knee joint, contributing to OA-like changes.

Various integrin molecules also affect TGFβ signaling such as integrin αvβ3 that enhances TGFβ-mediated collagen synthesis in cultured human kidney tubular cells, and integrin α2β1 that downregulates TGFβ synthesis assessed in the kidney cells of *itga2*-null mice (Hayashida *et al.* 2010; Girgert *et al.* 2010). Furthermore, in a cell culture model of glomerular injury *itga1*-null cells showed increased basal levels of SMAD2 and SMAD3 as well as significantly increased phosphorylated SMAD2 and SMAD3 compared to controls, indicative of increased fibrotic activity in the absence of integrin α1β1 (Chen *et al.* 2014). Interestingly, blocking TGFβ signaling with the TBRI-specific inhibitor SB43l542 ameliorated the *itga1*-null pro-fibrotic phenotype (Chen *et al.* 2014). Specific to cartilage, *itga1*-null chondrocytes are hypersensitive to the presence of TGFβ as demonstrated by increased activity of $[Ca^{2+}]_i$ transients as well as increased downstream activation of SMAD2/3 (Parekh *et al.* 2011). Therefore, the integrin-TGFβ signaling axis could alter joint cartilage homeostasis and therefore influence the progression of OA.

In addition to TBRII signaling, EGFR signaling has also been shown to contribute to the degradative changes in OA potentially through the influence of integrin α1β1. EGFR is a transmembrane receptor that is part of the ErbB family of receptor tyrosine kinases with a ligand-binding extracellular domain and a kinase domain that extends into the cytoplasm (Henriksen *et al.* 2013). Predominant ligands for EGFR include epidermal growth factor (EGF),

transforming growth factor α (TGFα), and heparin-binding EGF-like growth factor (HB-EGF) (Henriksen *et al.* 2013; Freed *et al.* 2017). Increased TGFα has been identified in synovial tissue of arthritic joints (Hallbeck *et al.* 2005) and has since been shown to increase catabolic activity in chondrocytes (Appleton *et al.* 2007). Upon ligand binding, EGFRs dimerize and auto-phosphorylate to induce activation and downstream signaling cascades (Figure 1; Freed *et al.* 2017). EGFRs present in articular chondrocytes are involved in the downstream production of reactive oxygen species (ROS) as well as catabolic proteinases (ie. ADAMTS5 and MMP13) (Zhang *et al.* 2014).

Upon activation through ligand binding and receptor dimerization, EGFR initiates various tyrosine kinase mediated downstream signaling pathways including MAPK/ERK, PI3K/Akt, SRC, PLCg/PKC, and JAK/STAT (Qin and Beier 2019). As these pathways are interconnected, activation of EGFR initiates a vast signaling cascade associated with a range of outcomes such as cell proliferation, differentiation, migration, and survival (Qin and Beier 2019). EGFR appears to play a dual role in articular cartilage, anabolically stimulating chondrocyte proliferation and survival, while catabolically suppressing the production of cartilage matrix components and stimulating the expression of catabolic enzymes and ROS (Figure 1; Qin and Beier 2019).

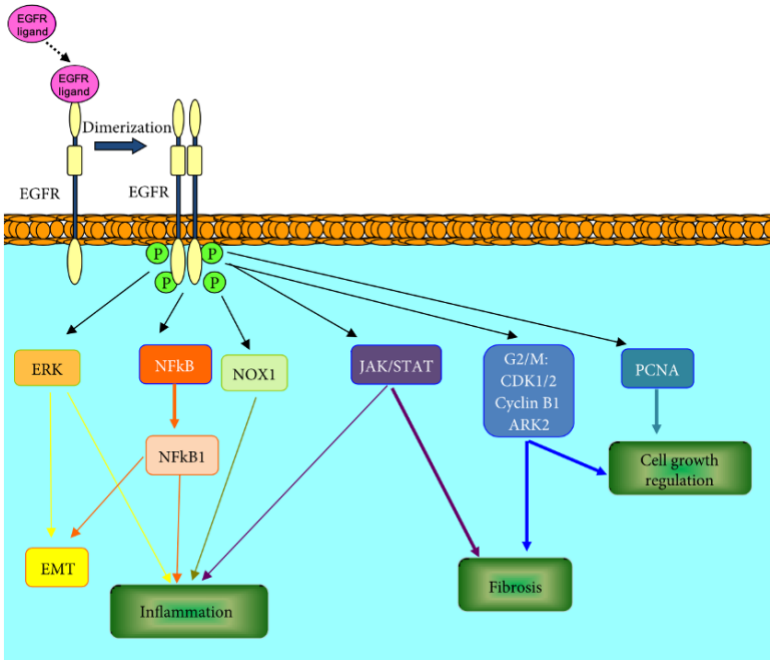

Figure 1: A portion of the EGFR activation pathway adapted from Rayego-Mateos *et al.* (2018) demonstrating the role of EGFR in both catabolic and anabolic processes within the cell, with the involvement in ROS production and inflammation being of particular interest to this thesis.

In the absence of EGFR, spontaneous cartilage degeneration develops in cartilage specific, conditional *Egfr*-null mice (Col2-Cre EgfrWa5/flox; sex not reported) at about 6 months of age (Jia *et al.* 2016). This is preceded by loss of superficial zone chondrocytes and proteoglycan content as well as disorganization of the collagen fibril network (Jia *et al.* 2016). Furthermore, post-traumatic OA induced with a DMM surgery results in rapid and severe OA development in these EGFR-deficient mice (Jia *et al.* 2016). Finally, the effect of EGFR activity on joint health has been evaluated through the endogenous EGFR inhibitor, mitogen-induced gene-6 (MIG-6) which is a scaffold protein that binds to EGFR and acts as a negative-feedback response to dampen EGFR signaling (Qin and Beier 2019). *Mig6*-null mice (ubiquitous deletion via genomic targeting vector; sex not reported) demonstrate increased activation of EGFR as well as joint overgrowth and malformation (Zhang *et al.* 2005). In another study using a cartilage

specific *Mig6*-deficient mouse model, spontaneous OA manifest as increased cartilage thickness and proteoglycan staining was reported, as well as osteophyte-like boney growth in the knees compared to controls (Pest *et al.* 2014). Furthermore, sex differences were accounted for but not present in this mouse model (Pest *et al.* 2014). Taken together, these studies suggest that the strict regulation of EGFR signaling is crucial for maintenance of joint homeostasis.

As previously described, integrin α1β1 suppresses EGFR activity through T-cell protein tyrosine phosphatase and as a result, EGFR activity is upregulated in *itga1*-null mice, leading to increased production of reactive oxygen species and catabolic enzymes, possibly contributing to an earlier onset of OA. In a similar vein, in mesangial cells, integrin α1β1 increases mRNA and protein levels of caveolin-1, a scaffolding protein involved in the formation of caveolae in cells contributing to receptor localization and signaling (Chen *et al.* 2010). This reduces phosphorylated EGFR levels and the associated ROS production (Chen *et al.* 2010). Furthermore, some studies investigating the influence of integrin α1β1 on EGFR signaling have revealed sex-dependent results. In their model of post-traumatic OA, Shin *et al.* (2016) saw that when a subset of the *itga1*-null and wild type mice were treated with the EGFR antagonist erlotinib, a protective effect was seen against boney signs of OA in the female mice, but dampening of EGFR had either no effect or was detrimental to males, and this result appeared to override any genotype effects (Shin *et al.* 2016). Other studies investigating sexual dimorphism in EGFR signaling has shown conflicting results. For example, Zhang *et al.* (2014) showed that suppressing the action of EGFR, either through genetic modification or use of the receptor antagonist gefitinib, resulted in increased cartilage degeneration following surgery to destabilize the medial meniscus, in male mice. However, in direct contrast to the results from Shin *et al.* and Zhang *et al.*, dampening of EGFR signaling via the tyrosine kinase inhibitor AG1478 actually

had protective effects in male rats against the development of post-traumatic OA (Appleton *et al.* 2015). Therefore, it is evident that EGFR plays a critical role in the maintenance of cartilage integrity in part through the influence of integrin $\alpha1\beta1$. In addition to direct manipulation of EGFR using genetic modifications and receptor antagonists, indirect measures of EGFR activity in cartilage, such as ROS production, provide indication of catabolic activity in the tissue.

1.5 Reactive Oxygen Species

ROS produced in the body are important for many physiological processes such as participating in the immune response to eliminate invading microbes and maintaining cardiovascular health through blood pressure regulation (Panday *et al.* 2015). ROS also have an important role in the pathogenesis of many diseases as oxidative stress is associated with inflammation and tissue damage (Touyz and Schiffrin 2004). ROS are biological derivatives of O_2 such as superoxide ($\cdot O_2^-$), hydrogen peroxide (H_2O_2), and hydroxyl anion (OH^-), as well as reactive nitrogen species, such as nitric oxide (NO), and peroxynitrite ($ONOO^-$) (Touyz and Schiffrin 2004). One of the major cellular sources of ROS is the nicotinamide adenine dinucleotide phosphate (NADPH) oxidases, also known as the NOX family (Segal and Abo 1993; Selvakumar *et al.* 2008). They form an enzyme complex that consists of the membrane-bound cytochrome b_{558} as well as cytoplasmic proteins, including $p47^{phox}$, that translocate to the cell membrane in response to cellular stimulation in order to produce superoxide (Segal and Abo 1993; Selvakumar *et al.* 2008). Over time, the ability for cells like chondrocytes to clear excess ROS diminishes, thereby tissue levels of oxidative stress increase with age (Jeon *et al.* 2018). Consequently, it is perhaps not surprising that elevated levels of ROS have been associated with the increase in EGFR signaling in *itga1*-null mice.

Studies in non-cartilaginous tissues show that through its influence on growth factor receptor signaling, integrin α1β1 negatively regulates ROS production (Chen *et al.* 2007; Chen *et al.* 2010). Assessment of the *itga1*-null model showed that cells and mice have increased basal levels of phosphorylated EGFR and associated profibrotic ROS production (Chen *et al.* 2007). Furthermore, in cell culture of primary mesangial cells, lack of integrin α1β1 also led to increased levels of phosphorylated caveolin-1, which occurs in response to oxidative stress in the cells (Borza *et al.* 2010; Chen *et al.* 2014). Finally, studies assessing the $p47^{phox}$ subunit of the NAPDH oxidase complex in a model of glomerular injury in *itga1*-null and wildtype mice showed that there is also increased phosphorylation of $p47^{phox}$ in *itga1*-null mesangial cells (Wang *et al.* 2015). When this $p47^{phox}$ subunit was knocked out, superoxide production was reduced, with a greater effect seen in the *itga1*-null cells compared to wild type (Wang *et al.* 2015). Taken together, these studies suggest that integrin α1β1 is important in the regulation of receptor tyrosine kinase activities that are involved in the production of ROS.

In addition to work carried out in the kidney, integrin α1β1 has also been associated with ROS production in chondrocytes. Previous work from our lab measured chondrocyte EGFR activity (superoxide production) *ex vivo* in intact mouse femora in response to the receptor antagonist erlotinib (Haskins 2018). Sexual dimorphism in chondrocyte superoxide production and the role of integrin α1β1 was reported, with chondrocytes from male mice having increased superoxide production compared to cells from females, and integrin α1β1 dampening superoxide production in chondrocytes from female but not male mice (Figure 2; Haskins 2018). Treatment with the EGFR inhibitor erlotinib resulted in significantly reduced superoxide production in *itga1*-null and wild type male mice but had the opposite effect on wild type female mice, and

there was no significant treatment effect on *itga1*-null female mice (Figure 2; Haskins 2018). Taken together these data highlight the role of integrin α1β1 in EGFR signaling and downstream ROS production in chondrocytes. Furthermore, these effects are sex dependent which may suggest a role for estrogen receptor signaling in the integrin-EGFR signaling axis.

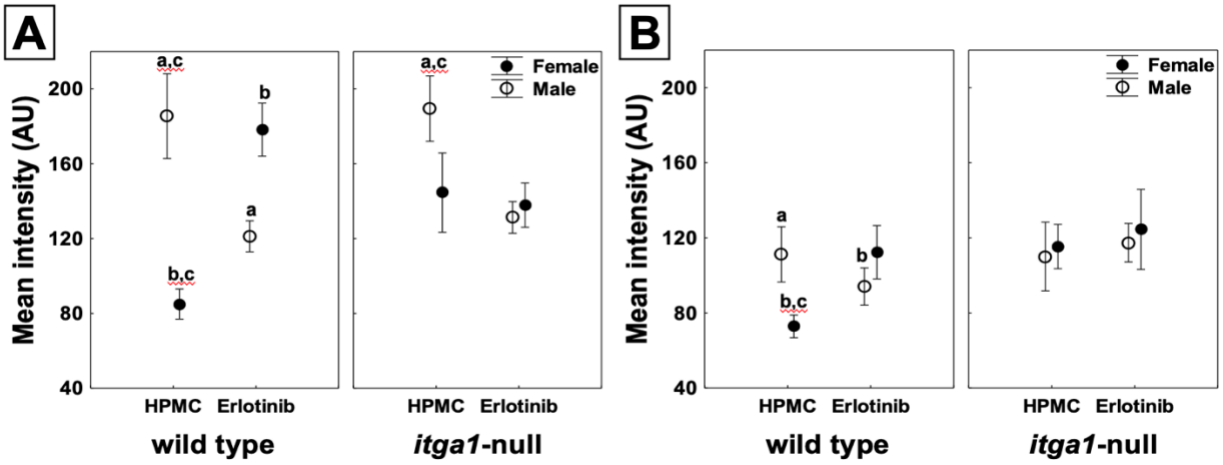

Figure 2: Mean intensity (arbitrary units) of 2-hydroxyethidium in femoral chondrocytes from the medial (A) and lateral (B) condyles of male and female wild type and *itga1*-null mice. Points are means (N = 3 femora, n = 90 cells) ± 95% CI. **a** Different from female equivalent (p £ 0.00023). **b** Different from *itga1*-null equivalent (p £ 0.025). **c** Different from erlotinib-treated equivalent (p £ 0.00015).

1.6 Estrogen Receptor

Emerging evidence indicates crosstalk between EGFRs and ERs, insinuating that ERs could be involved in the integrin-EGFR-mediated sex differences seen in chondrocyte signaling. In articular cartilage, estrogen can act through three ligand-dependent mechanisms and/or one ligand-independent mechanism (Roman-Blas *et al.* 2009). This ligand-independent pathway is connected to the development of spontaneous OA where growth factors such as epidermal growth factor (EGF) can activate ERs in the absence of ER ligands, like estradiol, and this crosstalk can occur in the cytoplasm and/or nucleus of cells (Roman-Blas *et al.* 2009). Therefore,

changes in EGFR activity, mediated by integrin α1β1, could influence ER expression and contribute to the sexual dimorphism of knee OA in *itga1*-null mice.

Physiologically, the primary active form of estrogen in the body, estradiol, elicits its effects through estrogen receptors (ERs), of which there are two isoforms, ERα and ERβ (Matthews and Gustafsson 2003). Both of the ER receptor isoforms (mRNA and/or protein levels) have been found in articular cartilage of various animal models such as rats, monkeys, cows, and pigs, as well as in human articular cartilage (Pelletier 2000; Richmond *et al.* 2000; Dayani *et al.* 1988; Claassen *et al.* 2001). Interestingly, studies have shown increased protein expression of ERs in females compared to males (Elbaradie *et al.* 2013), as well as decreased mRNA and protein expression of ERs in females compared to males (Van Der Eerden *et al.* 2002) assessed in cell cultures of isolated rat chondrocytes. This suggests a disparity between sexes in terms of ER expression patterns even on a molecular level, as well as discordance in the current literature. Increased expression in females could be due to the greater levels of systemic estrogen leading to increased ER gene expression, though the increased expression seen in males could ensure that they are more sensitive to changes in estrogen levels because they generally have less estrogen circulating systemically. Nevertheless, the current research seems to be inconclusive regarding expression patterns of ER in male versus female tissues and how this influences the development of OA, despite the evidence of the sexual dimorphism in this molecular signaling pathway.

Finally, a study by Sneikers and colleagues in 2009 saw that female mice carrying a deletion for either ERα or ERβ saw only mild cartilage damage and osteophyte formation, but when both receptors were simultaneously deleted, there was significantly increased osteophyte

formation as well as thinning of the subchondral plate. Although only assessed in female mice, this suggests that the deletion of one ER might be compensated for by the other, and/or they could be cooperating to elicit their cellular actions (Sniekers *et al.* 2009).

1.7 Research Gap, Hypothesis & Specific Aims

Integrin α1β1 is known to suppress EGFR activity via T-cell protein tyrosine phosphatase (Chen *et al.* 2007). Recent work from our lab has seen earlier cartilage damage in a post-traumatic model of OA (Shin *et al.* 2016), and more superoxide production (Haskins 2018) in *itga1*-null compared to wild type mice with sex-dependent effects of the EGFR antagonist, erlotinib. Together, these studies support the hypothesis that the protective role of integrin α1β1 in joint cartilage is mediated through suppression of EGFR activity. The sex-dependent effects of erlotinib further suggests that the influence of integrin α1β1 on EGFR signaling may be mediated by another major player, ERs. Disparity in ER expression in cartilage from males and females has been reported, however results are conflicting. In addition, crosstalk between ER and EGFR has been investigated but the mechanism of action is not well defined, and the influence of integrin α1β1 on ER expression has not been explored.

Therefore, the purpose of this thesis was to evaluate the expression of phosphorylated EGFR (pEGFR), 3-nitrotyrosine, and ERα and ERβ in the presence and absence of integrin α1β1 in knee chondrocytes. To this end immunohistochemistry was conducted using cryosections of femora and tibiae from *itga1*-null and wild type, male and female mice. We hypothesized that there would be increased expression of pEGFR and 3-nitrotyrosine in chondrocytes of *itga1*-null mice compared to wild type controls, and that this affect would be greater in females compared to males. Additionally, we hypothesized that there would be

increased expression of ERα and β in females compared to males, with a greater effect seen in the *itga1*-null compared to wild type mice.

2 Methods

2.1 Animals

All methods were approved by the University of Guelph Animal Care Committee (AUP#3655). Skeletally mature (18±2 weeks) *itga1*-null (Gardner *et al.* 1996) and wild type, female and male BALB/c mice (n=3 per group) were selected for experiments. Genotype was determined through a multiplex polymerase chain reaction (PCR) using DNA extracted from ear notches taken for identification. Mice were weighed (mean ± standard deviation; wild type female (28.0 ± 1.0g) and male (31.3 ± 2.2g), *itga1*-null female (27.5 ± 1.7g) and male (33.5g ± 1.8g)) then anesthetized with isoflurane and euthanized by cardiac puncture followed by cervical dislocation.

2.2 Cartilage Preparation

Femora and tibiae were isolated using micro-dissection, fixed overnight in 4% paraformaldehyde (Thermo Fisher Scientific, Mississauga, ON), decalcified for 32 hours (Cal-Ex II, Thermo Fisher Scientific, Mississauga, ON) and dehydrated (25% sucrose) overnight at 4°C. Femora were trimmed to two thirds their length and tibiae were cut midshaft before being embedded in cryomolds (15mm x 15mm x 5mm, VWR, Mississauga, ON) filled with optimal cutting temperature medium (Thermo Fisher Scientific, Mississauga, ON). In order to achieve a physiological orientation of the femur for sectioning, the shaft was balanced against the edge of the mold while the distal end was positioned in the center of the base of the mold with the condyles facing up. Tibiae were oriented flat in the base of the mold with the anterior side facing up. Cryosections (10µm) were cut in the coronal plane (CM 3050S, Leica Microsystems, Richmond Hill, ON) with four sections arranged on each microscope slide (Superfrost Plus,

Thermo Fisher Scientific, Mississauga, ON) and stored at -80°C until use. All slides selected for experiments were from the center of the joint, within the cartilage-cartilage contact region of the medial and lateral tibial plateaus and femoral condyles. Section quality (tissue flat to the slide, no folds or tears) was assessed using a brightfield microscope (Nikon Eclipse e400, Nikon, Mississauga, ON). Sections were then allocated to a treatment group (full antibody application, secondary only control, or blank control), with the best sections on each slide being assigned full antibody application.

2.3 Immunohistochemistry for 3-nitrotyrosine

Endogenous peroxidases were quenched (3% hydrogen peroxide in methanol) followed by additional blocking (4% normal horse serum) for one hour in a humidified chamber. Sections were then incubated with mouse monoclonal anti-nitrotyrosine antibody (1:500, ab61392, Abcam, Cambridge, MA) overnight at 4°C. The Ultra-Sensitive ABC Peroxidase Mouse IgG Staining Kit (Thermo Fisher Scientific, Mississauga, ON) was used for the application of the secondary antibody as well as the ABC complex. Sections were developed with 3-3'-diaminobenzidine (Sigma-Aldrich, Oakville, ON) and counterstained with hematoxylin for imaging using light microscopy.

2.4 Immunofluorescence for ERα, ERβ and pEGFR

Sections were blocked (5% normal goat serum) for one hour at room temperature. To determine the presence of ERα and ERβ, anti-ERα mouse monoclonal (1:200, MA5-13191) and anti-ERβ rabbit polyclonal (1:200, PA1-310B) primary antibodies (Thermo Fisher Scientific, Mississauga, ON) were diluted, mixed together, and applied to sections to incubate overnight at 4°C. Goat anti-mouse IgG (H+L) $F(ab')_2$ fragment Alexa Fluor 647 (1:500, A21237) and goat

anti-rabbit IgG (H+L) Alexa Fluor 555 (1:500, A21428) secondary antibodies (Thermo Fisher Scientific, Mississauga, ON) were then diluted, mixed together, and the sections incubated at room temperature for an hour. To determine the presence of pEGFR, anti-EGFR (phosphor 1092) rabbit monoclonal primary antibody (1:100, ab40815, Abcam, Cambridge, MA) and goat anti-rabbit IgG (H+L) Alexa Fluor 555 secondary antibody (1:500, A21428, Thermo Fisher Scientific, Mississauga, ON) were applied as described above. All sections were counterstained with 0.1M Hoechst 33342 (Invitrogen, Burlington, ON), coverslips applied (ProLong Gold, Thermo Fisher Scientific, Mississauga, ON) and sealed with nail polish.

2.5 Image Acquisition

For each experiment, images were taken from the medial and lateral femoral condyles and tibial plateaus of each mouse. For 3-nitrotyrosine, images of the stained tissue sections were captured using a Nikon Eclipse e400 microscope outfitted with a Nikon Coolpix 990 digital camera (Nikon, Mississauga, ON). Using the 40x/0.65 N.A. air objective lens, sequential images of the tissue sections were taken to capture the entire length and depth of the articular cartilage across both the medial and lateral femoral condyles/tibial plateaus. For ERα, ERβ, and pEGFR a single confocal image in the central cartilage-cartilage contact region of each medial/lateral tibial plateau/femoral condyle was captured using a 40x/0.75-1.25 N.A. oil objective (Leica DM 6000B confocal microscope with a TCS SP5 scanner system, Leica Microsystems, Richmond Hill, ON). Image resolution was set to 2048x2048 pixels with a two-line average and an optical slice thickness of 7.419 μm. A brightfield image and sequential fluorescent scans were captured to avoid interference between the florescent dyes. The following excitation and emission settings

were used for each dye; ERα (ex 633nm, em 670-720nm), ERβ and pEGFR (ex 543nm, em 570-600nm or 625-640 respectively) and Hoechst (ex 405nm, em 440-460nm).

2.6 Image Analysis & Statistics

For 3-nitrotyrosine, images were merged to create a collage of each femoral condyle/tibial plateau and the tidemark was marked using the 'draw' tool (PowerPoint). Collages of each sample were randomized and the total number of chondrocytes in the full depth articular cartilage, and those stained positively for 3-nitrotyrosine were manually quantified by two blinded graders. Zonal analysis was not possible as the zones could not be distinguished in the thin femoral cartilage (20-30μm, 3-4 cell layers). For ERα, ERβ, and pEGFR, the tide mark and articular surface of the cartilage seen on the DIC images were marked on the fluorescent images (ImageJ, National Institutes of Health, Maryland, United States) and saved and randomized as .tiff files ready for counting. For the majority of sections stained for ERα and ERβ, one image with all color channels was used. In some instances, images with identical x-y coordinates were taken in different z-planes in the red or green channels and were merged together to enhance the staining and minimize the background fluorescence on the final image. The total number of chondrocytes and those stained positively for ERα alone, ERβ alone, both ERα and β or pEGFR were manually counted by two blinded graders and tallied electronically (ImageJ, National Institutes of Health, Maryland, United States). Pearson correlations were run between the data sets from the two graders. Pearson correlation coefficients of 0.97 for pEGFR counts, 0.88 for 3-nitrotyrosine counts, and 0.97 for ERα and β counts were obtained and therefore the cell counts of the two graders were averaged and percent positive cells was calculated (Salkind 2010). An ANOVA (3-nitrotyrosine and pEGFR data) or a repeated measures ANOVA (ER data) with sex

(male/female), genotype (*itga1*-null/wild type), bone (femur/tibia) and condyle (medial/lateral) as factors were conducted (Statistica™, Tibco, Palo Alto, CA). Fisher LSD post hoc tests were conducted where appropriate and significance was set at $p<0.05$.

3 Results

3.1 Animals

As expected, male mice were 4.5g heavier ($p < 0.0001$) than female mice (males = 32.3 ± 2.3g; females = 27.9 ± 1.4g (mean ± SD)) and genotype did not affect mass (data not shown).

3.2 pEGFR Immunofluorescence

Chondrocytes stained positively for pEGFR throughout cartilage depth across the tibial plateaus and femoral condyles relative to secondary only control sections (Figure 3).

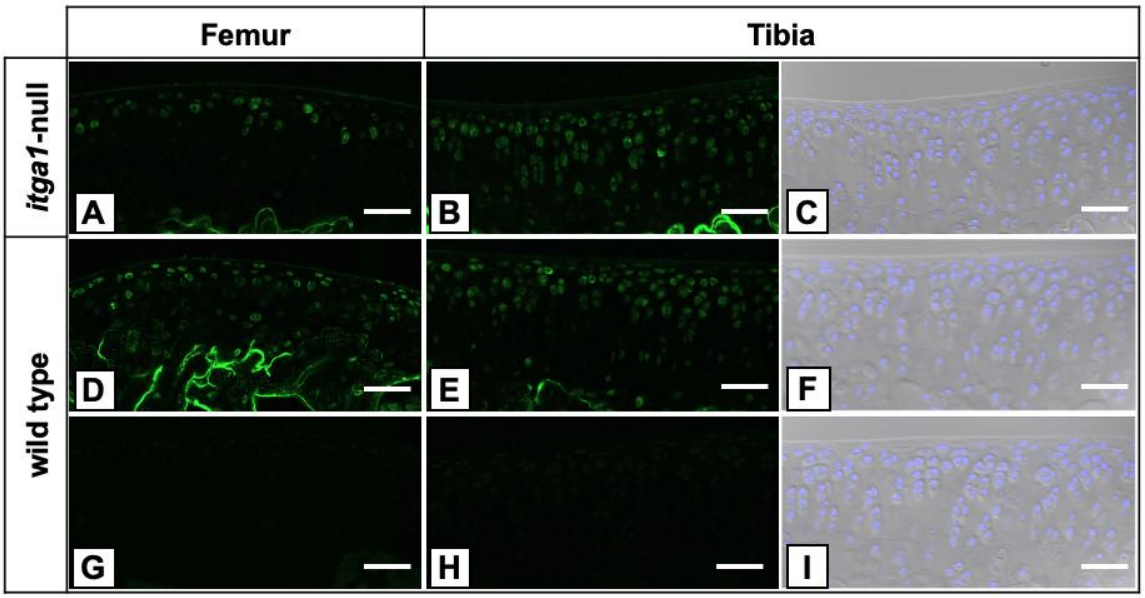

Figure 3: Confocal microscopy images of femoral (A,D,G) and tibial (B,C,E,F,H,I) cryosections showing articular cartilage from the lateral compartment of *itga1*-null (A-C) and wild type (D-I) male mice immunostained green for pEGFR (A,B,D,E). Nuclei were counterstained blue with Hoechst as seen in the DIC images (C,F,I). Secondary antibody only control sections (G,H) show negligible autofluorescence from the cartilage. Scale bar 50 μm.

Chondrocyte expression of pEGFR was affected by a genotype and bone interaction ($p = 0.014$) (Figure 4). Specifically, 15% more *itga1*-null chondrocytes stained positively for pEGFR on the tibial plateaus compared to the femoral condyles ($p = 0.000009$), but there was no bone effect in wild type mice. Furthermore, 8% more femoral chondrocytes stained positively for

pEGFR in wild type compared to *itga1*-null mice (p = 0.01426), however there was no genotype effect in the tibia. Sex had no influence upon chondrocyte expression of pEGFR.

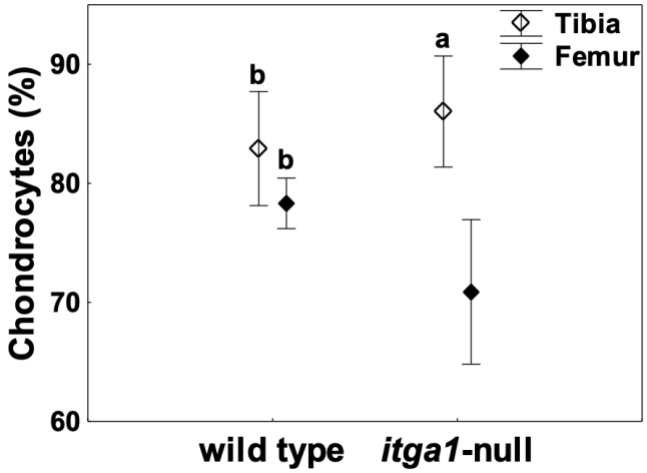

Figure 4: Percent of chondrocytes stained positively for pEGFR as a function of genotype and bone. Data points are means (N = 6, n ≥ 820 or 1560 cells for femur or tibia respectively) ± 95% CI. **a** Different from femur equivalent (p = 0.000009). **b** Different from *itga1*-null femur (p < 0.01426).

3.3 3-nitrotyrosine Immunohistochemistry

Chondrocytes stained positively for 3-nitrotyrosine throughout cartilage depth across the tibial plateaus and femoral condyles relative to secondary only control sections (Figure 5).

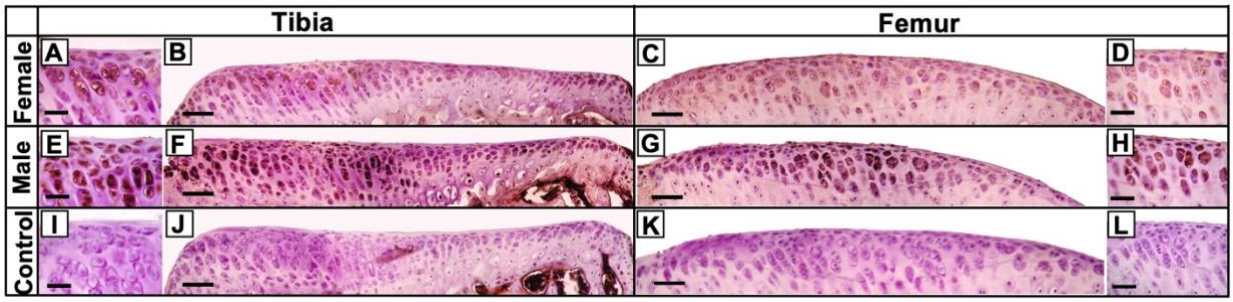

Figure 5: Light microscopy images of the full thickness articular cartilage of the medial tibial plateau or femoral condyle from female (A-D) or male (E-L) wild type mice. Sections are peroxidase stained for 3-nitrotyrosine (A-H) or secondary only control (I-L). Scale bar 20µm (A,D,E,H,I,L) or 50µm (B,C,F,G,J,K). Note the increased staining in tissues from male compared to female mice.

On average, males had 10% more chondrocytes stained positively for 3-nitrotyrosine compared to females (p=0.009) (Figures 5 and 6). Genotype, bone and compartment did not affect 3-nitrotyrosine staining (data not shown).

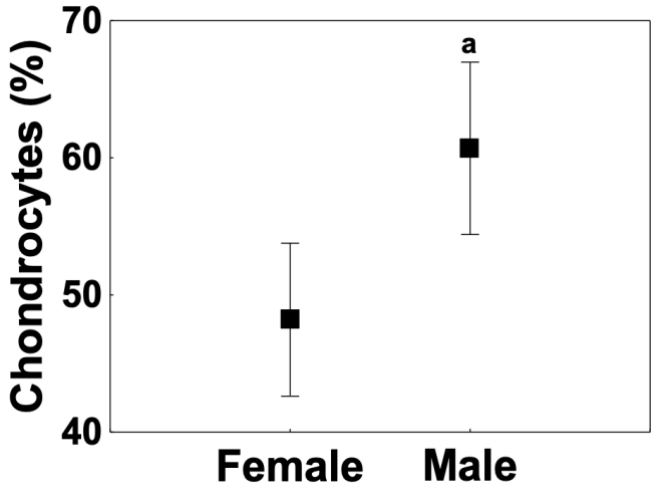

Figure 6: Percent of chondrocytes stained positively for 3-nitrotyrosine as a function of sex. Data points are means (N = 6, n ≥ 8860 cells) ± 95% CI. **a** Significantly different from female (p=0.009).

3.4 Estrogen Receptor Immunofluorescence

Chondrocytes stained positively for ERα and β throughout cartilage depth across the tibial plateaus and femoral condyles relative to secondary only control sections (Figure 7). ERα and β were present in the nucleus as well as the cytoplasm of chondrocytes and the receptors were sometimes colocalized in the cytoplasm (Figure 8).

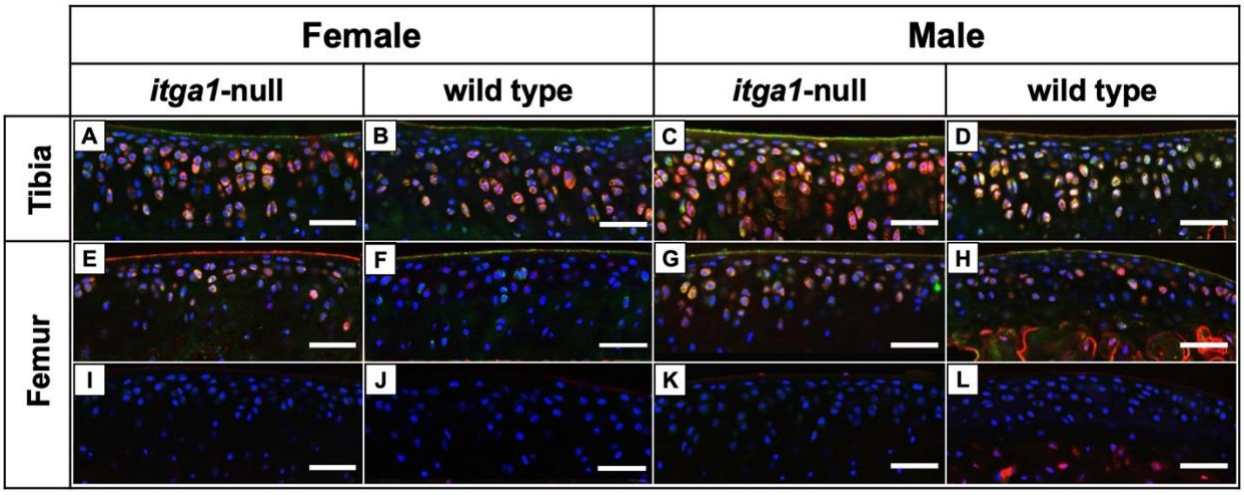

Figure 7: Confocal microscopy images of full thickness articular cartilage from the lateral tibial plateau (A-D) and medial femoral condyle (E-L) of female and male *itga1*-null and wild type mice. Chondrocytes stained red for ERα (A-H), green for ERβ (A-H) or secondary only controls (I-L). All counterstained blue with Hoechst (A-L). Scale bar 50µm.

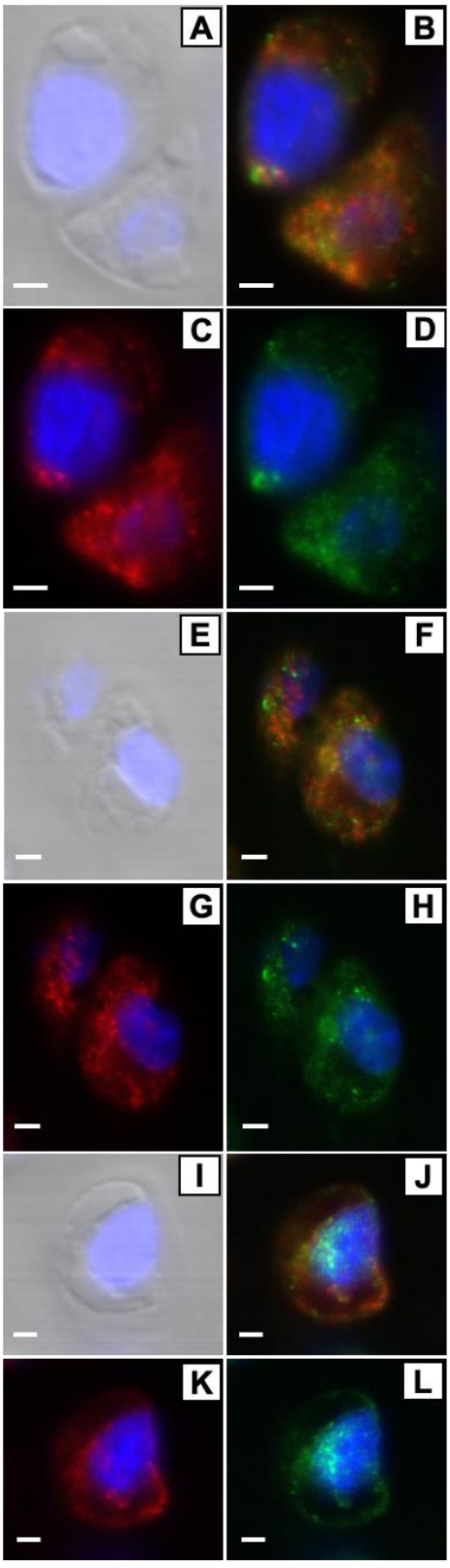

Figure 8: Digitally zoomed confocal microscopy images of chondrocytes from the lateral tibial plateaus of female wild type (A-D), female *itga1*-null (E-H), and male *itga1*-null (I-L) mice. Images show DIC (A,E,I), ERα stained red (C,G,K), ERβ stained green (D,H,L) or overlay of ERα and β (B,F,J). All nuclei counterstained blue with Hoechst. Note the presence of ERα and ERβ in the cytoplasm (C,G,K;D,H,L) and nuclei (G,K;H,L) and colocalization of ERα and β in the cytoplasm (B,F,J). Scale bar 2 μm.

The percent of chondrocytes stained positively for ERs was influenced by sex ($p = 0.028$) as well as a genotype and bone interaction ($p = 0.004$). In the tibia (Figure 9A), the percent of chondrocytes stained positively for both ERα and β was at least 40% greater than either receptor alone or no receptor, independent of genotype and sex ($p < 0.000603$). This expression pattern was also observed in femoral chondrocytes (Figure 9B) from male and female *itga1*-null mice ($p < 0.00003$) and male wild type mice ($p < 0.0055$). In femoral chondrocytes from female wildtype mice however, similar numbers (40%) of chondrocytes were stained positively for either ERβ alone or both ERα and β.

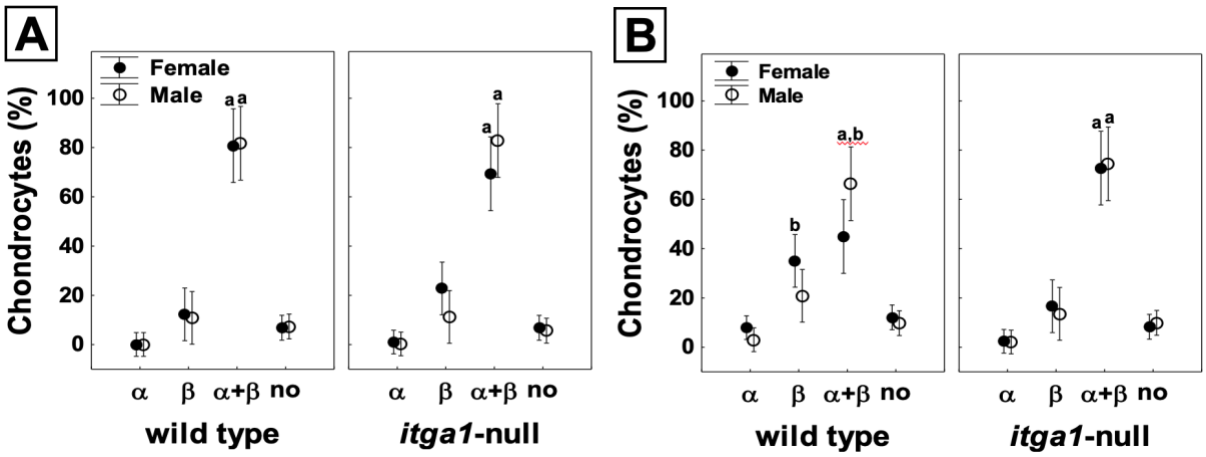

Figure 9: Percent of tibial (A) and femoral (B) chondrocytes stained positively for ERα, ERβ, ERα + β, or no receptor as a function of genotype and sex. Note the expression of ERα + β is significantly greater than either receptor alone or no receptor, except in femoral chondrocytes from wild type females. Data points are means ($N = 3$, $n \geq 400$ or 850 cells for femur or tibia respectively) ± 95% CI. **a** Significantly different from all sex equivalent receptor combinations ($p < 0.000001$). **b** Significantly different from sex equivalent ($p = 0.002234$).

4 Discussion

The purpose of this thesis was to assess the percent of murine knee chondrocytes stained positively for pEGFR, 3-nitrotyrosine, and ERα and ERβ in the presence and absence of integrin α1β1. We showed that integrin α1β1 had limited influence on the percent of chondrocytes stained positively for pEGFR or 3-nitrotyrosine. In contrast, we found that integrin α1β1 did influence ERα and β expression that were co-expressed as well as co-localized in chondrocytes. Finally, we show sexual dimorphism in 3-nitrotyrosine production, but surprisingly not in pEGFR expression.

Firstly, contrary to our hypothesis, we show that integrin α1β1 only increased the percent of chondrocytes stained positively for pEGFR in the femur (by 8%) but had no effect in the tibia or on the percent of chondrocytes stained positively for 3-nitrotyrosine. In a model of glomerular injury, integrin α1β1 has been shown to suppress EGFR activity via T-cell protein tyrosine phosphatase (Chen *et al.* 2007). In agreement with this, previous work from our lab saw earlier cartilage damage in *itga1*-null compared to wild type mice following surgery to destabilize the medial meniscus, which was ameliorated with an EGFR antagonist, though only in female mice (Shin *et al.* 2016). Furthermore, *itga1*-null chondrocytes have more superoxide production compared to their wild type counterparts when measured *ex vivo* in murine femora, but again only in female mice (Haskins 2018). Together, these studies provide additional evidence to support the protective role of integrin α1β1 in cartilage through suppression of EGFR activity, however our current results do not support this hypothesis. The divergence of our current results may be reflective of our use of a subclinical as opposed to a surgical intervention model of OA in mice, and the contrasting measures of ROS production; 3-nitrotyrosine and 2-hydroxyethidium.

Whereas 3-nitrotyrosine is an *in situ* indirect measure of ROS (the byproduct of superoxide reacting with nitric oxide and then with proteins (Lepetsos and Papavassiliou 2016)), 2-hydroxyethidium is an *ex vivo* fluorescent product of a direct reaction between the small molecule dihydroxyethidium and superoxide (Wang *et al.* 2013). Thus, the lack of surgical intervention and indirect measure of ROS may have hampered our ability to measure a genotypic effect in pEGFR and ROS.

The sex-specific alterations in EGFR signaling in *itga1*-null mice reported in our previous work (Shin *et al.* 2016; Haskins 2018) might suggest that, in addition to T-cell protein tyrosine phosphatase (Chen *et al.* 2007), the influence of integrin α1β1 on EGFR signaling may be mediated by another major player, ERs. In fact, ER activation has been shown to promote the association of a complex between EGFR, ERα, and the kinase Src (Migliaccio *et al.* 2006). Additionally, ERα has been shown to upregulate EGFR expression and activation in cell culture (Migliaccio *et al.* 2006) and ERα expression correlates with the severity of facet joint arthritis in post-menopausal women (Ha *et al.* 2005). Finally, EGF-induced DNA synthesis and transcription as well as lipid turnover in the uterus of ovariectomized mice were prevented by the ER antagonist ICI 164,384 (Ignar-Trowbridge *et al.* 1992) and absent from ERα-deficient mice (Curtis *et al.* 1996). Taken together, these studies demonstrate the dependency of EGF action on ERα in reproductive organs and cell culture models. Therefore, it is possible that integrin α1β1 may exert its influence on chondrocyte EGFR indirectly through ER, rather than solely through T cell protein tyrosine phosphatase.

To this end, the data in this thesis does suggest that integrin α1β1 influences ERα and β expression and thus may impact EGFR signaling indirectly. Specifically, we show that cartilage

from female wild type femora had approximately 20% more chondrocytes stained positively for ERβ alone, compensated for by 20% fewer chondrocytes stained positively for both ERα and β. In agreement with our data, it has been shown that cells induced to express ERβ increased integrin α1β1 mRNA and protein content as well as increased adhesion to extracellular matrix components such as laminin in a breast cancer culture model (Lindberg *et al.* 2010). Interestingly however, the *in vitro* treatment of endometrial cells with estrogen had no effect on the expression of various integrin molecules, including integrin α1β1 (Sillem *et al.* 1997). These studies together with our findings suggest that integrin α1β1 and ERβ can influence each other's expression and activation, independently of estrogen, and thus integrin α1β1 may influence EGFR signaling through both T-cell protein tyrosine phosphatase and ERβ.

Independent of the effects of integrin α1β1 on ER expression, we observed that the vast majority (80%) of chondrocytes express both ERα and β and that these receptors are often colocalized and are present at the cell surface, in the cytoplasm and in the nucleus of chondrocytes. Our data are consistent with other reports of the distribution of the ER isoforms in both the nucleus and cytoplasm in various models including rats and cultured human chondrocytes (Ushiyama *et al.* 1999; Nilsson *et al.* 1999; Oshima *et al.* 2007) however we show their colocalization in chondrocytes for the first time. It is known that both ligand-dependent and -independent ER activity can influence chondrocyte biological activity, and that ER can translocate to the nucleus to influence gene expression in chondrocytes (Roman-Blas *et al.* 2009). ERα and β form homodimers and/or heterodimers upon activation (Pettersson and Gustafsson 2001) and bind to the same specific DNA sequences (estrogen response elements) *in vitro*, thus jointly regulating DNA transcription in the nucleus in response to activation (Hyder *et*

al. 1999; Klinge 2000). Together with our work, this implies that through co-localization of the two dominant isoforms, the receptors may act cooperatively to elicit their cellular actions (Sneikers *et al.* 2009).

While genotype effects were absent, we did observe sexual dimorphism in chondrocytes stained for 3-nitrotyrosine, with more chondrocytes stained positively for 3-nitrotyrosine in male compared to female cartilage (about 10%). This is in agreement with our previous work measuring superoxide production *ex vivo* in murine femora that saw increased chondrocyte ROS production in untreated chondrocytes from males compared to females (Haskins 2018). Additional studies in chondrocytes are lacking, however antioxidant enzyme activity in various organs are increased in females compared to males (Chen *et al.* 2011), and evidence in non-cartilaginous tissues supports increased ROS production in males compared to females such as in the analysis of human blood samples (Ide *et al.* 2002), and *in vivo* measurements in the microvessels of hypertensive rats (Dantas *et al.* 2004). In contrast to our 3-nitrotyrosine result and contrary to our hypothesis, sexual dimorphism was absent in our measurements of pEGFR. This is in contrast to our previous work that saw increased pEGFR expression in male compared to female mice 12 weeks following DMM surgery (Shin *et al.* 2016). As the same antibody was used in both experiments, this disparity is likely due to surgery exacerbating the sexual dimorphism making it measurable in the post-traumatic OA model but not in our subclinical model. Taken together, this evidence suggests that activation of EGFR is stimulated by an injurious or traumatic event, potentially affecting chondrocyte ROS production and thus cartilage degradation in a sex-dependent manner.

Finally, both genotypic effects observed in pEGFR and ER expression are present in femoral but not tibial cartilage. This could be explained by the differential mechanical stimuli

experienced by tibial compared to femoral chondrocytes and their integrins during gait, as tibial cartilage and chondrocytes are exposed to more consistent static loading compared to the more intermittent, cyclic loading of femoral chondrocytes (Clark *et al.* 2005). At the molecular level, compression results in collagen fibrils tugging on the integrin receptors on the surfaces of chondrocytes (Kechagia *et al.* 2019); as such, integrins on tibial chondrocytes may experience a more sustained tug compared to a cyclical tugging and relaxing of femoral integrins during the gait cycle. It is known that mechanical force strengthens the adhesions of integrins to the extracellular matrix, whereas relaxation weakens these adhesions and accelerates dissociation (Puklin-Faucher and Sheetz 2009). Furthermore, tyrosine phosphorylation of signaling proteins and MAPK activity associated with the α2 and β1 integrin subunits are more pronounced in osteoblasts under cyclic compared to continuous mechanical stress (Schmidt *et al.* 1998). Thus, under a consistent static load, integrin molecules remain activated due to stronger interactions with their ligands in the extracellular matrix, however while experiencing intermittent cyclic loading integrins are periodically being activated and deactivated based on the conformational changes of their environment, as well as the receptors themselves. Consequently, it would make sense that the influence of integrin α1β1 on the expression of pEGFR and ERα and β would be more pronounced in femoral compared to tibial chondrocytes.

4.1 Strengths & Limitations

In this thesis we have shown for the first time that integrin α1β1 influences EGFR and ER expression in murine articular cartilage in a location-dependent manner. Assessment of both the femur and tibia allowed us to observe sex and genotypic effects in the femur but not the tibia in both experiments. Additionally, we have demonstrated that ERα and ERβ co-localize together

in chondrocytes using immunofluorescence and confocal microscopy. Our double staining with contrasting fluorescent probes and the high sensitivity and resolution afforded by confocal microscopy allowed for the novel detection of the two receptors together in the nucleus, cytoplasm, and at the cell surface of articular chondrocytes.

The primary interest of this work was to understand the influence of the collagen receptor integrin α1β1 on the expression of pEGFR, 3-nitrotyrosine, and ERα and ERβ. This was achieved using immunohistochemical techniques to stain *in situ* cryosections taken from the knees of *itga1*-null female and male mice. Integrin α1β1, EGFR, ERα and ERβ are transmembrane receptors found on the surface of chondrocytes and in the case of integrin α1β1 is directly connected to the extracellular matrix. Thus, it was critical to our experiments that the cell membrane and its immediate interaction with the extracellular matrix be preserved. This was achieved through the use of the *itga1*-null mouse that enabled us to delete integrin α1β1 *in vivo* and by processing intact femora and tibiae from female and male mice for cryosectioning. The small size of the mouse further enabled medial and lateral differences of the intact femoral and tibial cartilages to be assessed on the same section thus limiting the variability in our interpretation of immunohistochemical results. To best preserve our proteins of interest, we utilized fixed frozen sections to limit fixation, decalcification and processing procedures that might damage the integrity of the chondrocyte/extracellular matrix interaction and the antigens of interest. Finally, our choice of secondary antibodies and staining techniques allowed for amplification of the antibody signal and thus detection of the smaller molecules and receptors, and imaging with confocal microscopy enabled us to stain and analyze ERα and β together using contrasting fluorophores and sequential scanning.

While there are a number of advantages to the current study, there are also some notable limitations. Firstly, our use of the *itga1*-null mouse introduces variation to the sample population that would not be present in cell culture and which could decrease the power of the results. Additionally, the ubiquitous deletion of the α1 subunit of integrin α1β1 means that this receptor is deleted in all tissues throughout the body of these mice. This includes tissues that may influence cartilage homeostasis such as bone, synovium, ligaments, muscles, menisci, etc., and thus may influence the results of our work. Furthermore, the quality of immunohistochemistry is heavily dependent on the primary antibody used. Antibodies that are more specific and reliable are able to sufficiently bind the target molecule while minimizing background staining, leading to more accurate results. In our case, the pEGFR antibody was not as strong as the ERα and β antibodies, though still produced quantifiable staining. We were, however, unable to measure EGFR (inactivated) along with the pEGFR due to the poor quality of the available antibodies. Moreover, although the different cartilage-cartilage contact sites of the knee (medial/lateral femoral condyles/tibial plateaus) were represented, only one slide was stained from each location. While that slide taken from the middle of the cartilage-cartilage contact region may represent all sections from the contact region of that site of the knee, it may not represent more peripheral regions of the cartilage that are covered by meniscus. Furthermore, although the experimental design did allow for multiple controls on each slide, more slides immunostained from each joint would potentially give a better representation of the number of chondrocytes positively stained for pEGFR, 3-nitrotyrosine, as well as ERα and β in murine knee cartilage. Finally, numerous processes in the body result in ROS production, including activated neutrophils and macrophages in inflammatory immune responses as well as fibroblasts, vascular smooth muscle cells, cardiac myocytes, and endothelial cells for regulation of their respective

intracellular signaling cascades (Valko *et al.* 2007). Therefore, assessment of 3-nitrotyrosine as a measure of ROS production could be the result of a number of endogenous sources of ROS, not solely EGFR. However, the measurement of pEGFR and 3-nitrotyrosine production in tandem allows for more direct conclusions to be drawn from our results.

4.2 Clinical Applications & Future Directions

With the advantages and disadvantages of the study in mind, the clinical significance of the role of integrin α1β1 in the regulation of EGFR and ER activity can be discussed. Previous work from our lab supports the hypothesis of integrin α1β1 playing a protective role against the progression of OA through suppression of EGFR activity. Although the direct influence of integrin α1β1 on EGFR signaling was muted in the current study, the influence of integrin α1β1 on ERβ was seen in chondrocytes from female mice with a biologically significant shift in the ER expression pattern (about 20%). This suggests that ERs may act as another way for integrin α1β1 to influence EGFR signaling in chondrocytes, potentially contributing to the sexual dimorphism seen in the results of our previous work and generally to OA progression. As such, the present study provides new evidence in support of integrin α1β1 as a potential drug target in the prevention and treatment of OA.

Generally, understanding the underlying molecular mechanisms implicated in the development of OA is essential for the development of effective, targeted treatment strategies. Furthermore, defining OA in its earliest stages will allow for timely interventions to hopefully modify the course of the disease. The apparent sexual dimorphism seen generally in OA pathogenesis and more specifically in the integrin α1β1-EGFR-ER signaling axis indicates the potential need for more individualized, sex-dependent treatments. In the age of personalized

medicine, this approach would yield better health outcomes, increase the efficacy of treatments, and reduce adverse drug reactions for OA patients.

With this in mind, future work will need to continue to investigate the role of estrogen and ER signaling in the integrin α1β1-EGFR paradigm. Firstly, ER expression patterns should be assessed as we have done *in situ* with immunofluorescence but in a spontaneous OA (aged mice) or post-traumatic OA (ie. DMM) model. The OA-induced damage to knee cartilage and other tissues could stimulate a more pronounced effect that could lead to a better understanding of the role of estrogen in knee cartilage homeostasis and OA pathogenesis. Subclinically, we have shown that the significant changes to ER expression occur in the femur, thus this effect, along with the sex and genotype differences could be exacerbated in an OA model. Furthermore, studies utilizing live cell imaging of male and female murine femora *ex vivo* would allow for real-time measurements of chondrocyte ROS production (via 2-hydroxyethidium) in response to estrogen treatment. Treating the femora with isoform-specific ER antagonists such as methylpiperidinopyrazole for ERα (Zhou *et al.* 2009) or 2-phenyl-3-(4-hydroxyphenyl)-5,7-bis(trifluoromethyl)-pyrazolo[1,5-α]pyrimidine for ERβ (Compton *et al.* 2004), with and without estrogen treatment would unveil the specific contributions of ERα and β to chondrocyte ROS production. Finally, these *ex vivo* experiments could be performed in wild type and *itga1*-null mice to define the influence of integrin α1β1 on estrogen signaling specifically in articular cartilage. As previous work has seen increased integrin α1β1 mRNA and protein expression as well as receptor activity with expression of ERβ (Lindberg *et al.* 2010), it is reasonable to think that the proposed experiments would result in more superoxide production in wild type compared to *itga1*-null femora and that treatment with ER antagonists would ameliorate these

effects. Furthermore, taking our results into consideration, there might be a greater effect of estrogen treatment on females compared to males due to the differences in receptor localization.

4.3 Conclusion

In conclusion, we show that integrin α1β1 had limited influence on the percent of chondrocytes stained positively for pEGFR or 3-nitrotyrosine. In contrast we found that integrin α1β1 did influence ERα and β expression and show for the first time that they are co-localized as well as co-expressed in chondrocytes. Finally, sexual dimorphism was identified in chondrocyte 3-nitrotyrosine production, but surprisingly not in pEGFR expression. Future work must focus on the role of estrogen and ER signaling in the maintenance of chondrocyte homeostasis *in situ* with histological analysis of an OA model, as well as live cell imaging of *ex vivo* chondrocyte responses to modulation of estrogen signaling in wild type and *itga1*-null mice.

REFERENCES

Abulhasan, J. F., & Grey, M. J. (2017). Anatomy and physiology of knee stability. *Journal of Functional Morphology and Kinesiology*, *2*(4). https://doi.org/10.3390/jfmk2040034

Ahsan H. (2013). 3-Nitrotyrosine: A biomarker of nitrogen free radical species modified proteins in systemic autoimmunogenic conditions. *Hum Immunol*. doi:10.1016/j.humimm.2013.06.009

Andriacchi, T. P. (1994). Dynamics of knee malalignment. *The Orthopedic Clinics of North America*, *25*(3), 395—403. Retrieved from http://europepmc.org/abstract/MED/8028883

Appleton, C. T. G., Usmani, S. E., Bernier, S. M., Aigner, T., & Beier, F. (2007). Transforming growth factor α suppression of articular chondrocyte phenotype and Sox9 expression in a rat model of osteoarthritis. *Arthritis and Rheumatism*, *56*(11), 3693–3705. https://doi.org/10.1002/art.22968

Appleton, C. T. G., Usmani, S. E., Pest, M. A., Pitelka, V., Mort, J. S., & Beier, F. (2015). Reduction in disease progression by inhibition of transforming growth factor α-CCL2 signaling in experimental posttraumatic osteoarthritis. *Arthritis & Rheumatology (Hoboken, N.J.)*, *67*(10), 2691–2701. https://doi.org/10.1002/art.39255

Arden, E., Hunter, D., Arden, N. (2008). Osteoarthritis. 6th ed. Oxford: OUP Oxford.

Arden, N., Nevitt, M.C. (2006). Osteoarthritis: Epidemiology. *Best Pract Res Clin Rheumatol*. 20(1): 3-25.

Bakker, A. C., van de Loo, F. A. J., van Beuningen, H. M., Sime, P., van Lent, P. L. E. M., van der Kraan, P. M., … van den Berg, W. B. (2001). Overexpression of active TGF-beta-1 in the murine knee joint: Evidence for synovial-layer-dependent chondro-osteophyte formation. *Osteoarthritis and Cartilage*, *9*(2), 128–136. https://doi.org/10.1053/joca.2000.0368

Benninghoff, A. (1925). Form und Bau der Gelenkknorpel in ihren Beziehungen zur Funktion. *Zeitschrift Für Anatomie Und Entwicklungsgeschichte*, *76*(1–3), 43–63. https://doi.org/10.1007/bf02134417

Borza, C. M., Chen, X., Mathew, S., Mont, S., Sanders, C. R., Zent, R., & Pozzi, A. (2010). Integrin α1β1 promotes caveolin-1 dephosphorylation by activating T cell protein-tyrosine phosphatase. *Journal of Biological Chemistry*, *285*(51), 40114–40124. https://doi.org/10.1074/jbc.M110.156729

Bowman, K. F., & Sekiya, J. K. (2009). Anatomy and Biomechanics of the Posterior Cruciate Ligament and Other Ligaments of the Knee. *Operative Techniques in Sports Medicine*, *17*(3), 126–134. https://doi.org/10.1053/j.otsm.2009.07.001

Broom, N. D., & Myers, D. B. (1980). A study of the structural response of wet hyaline cartilage to various loading situations. *Connective Tissue Research*, *7*(4), 227–237. https://doi.org/https://doi.org/10.3109/03008208009152358

Brouwer, G.M., Val Tol, A.W., Bergink, A.P., Bersen, B. J. N., Reijman, M., Pols, H.A.P., Bierma-Zeinstra, S.M.A. (2007). Association between valgus and varus alignment and the development and progression of radiographic osteoarthritis of the knee. *Arthritis Rheumatol*. 56(4): 1204-11.

Buckwalter, J. A., & Mankin, H. J. (1997). Instructional Course Lectures, The American Academy of Orthopaedic Surgeons - Articular Cartilage. Part I. *The Journal of Bone & Joint Surgery*, *79*(4), 600–611. https://doi.org/10.2106/00004623-199704000-00021

Chen, X., Abair, T. D., Ibanez, M. R., Su, Y., Frey, M. R., Dise, R. S., … Pozzi, A. (2007). Integrin α1β1 Controls Reactive Oxygen Species Synthesis by Negatively Regulating Epidermal Growth Factor Receptor-Mediated Rac Activation. *Molecular and Cellular Biology*, *27*(9), 3313–3326. https://doi.org/10.1128/mcb.01476-06

Chen, Y., Ji, L. L., Liu, T. Y., & Wang, Z. T. (2011). Evaluation of gender-related differences in various oxidative stress enzymes in mice. *Chinese Journal of Physiology*, *54*(6), 385–390. https://doi.org/10.4077/CJP.2011.AMM080

Chen, X., Wang, H., Liao, H. J., Hu, W., Gewin, L., Mernaugh, G., … Pozzi, A. (2014). Integrin-mediated type II TGF-β receptor tyrosine dephosphorylation controls SMAD-dependent profibrotic signaling. *Journal of Clinical Investigation*, *124*(8), 3295–3310. https://doi.org/10.1172/JCI71668

Chen, X., Whiting, C., Borza, C., Hu, W., Mont, S., Bulus, N., … Pozzi, A. (2010). Integrin α1β1 Regulates Epidermal Growth Factor Receptor Activation by Controlling Peroxisome Proliferator-Activated Receptor γ-Dependent Caveolin-1 Expression. *Molecular and Cellular Biology*, *30*(12), 3048–3058. https://doi.org/10.1128/mcb.00892-09

Claassen, H., Hassenpflug, J., Schunke, M., Sierralta, W., Thole, H., Kurz, B. (2001). Immunohistochemical detection of oestrogen receptor alpha in articular chondrocytes from cows, pigs and humans: in situ and in vitro results. *Ann Anat*. 183:223–7.

Clark, A. L. (2008). Osteoarthritis: What we have been missing in the patellofemoral joint. *Exercise and Sport Sciences Reviews*, *36*(1), 30–37. https://doi.org/10.1097/jes.0b013e31815e4217

Clark, A. L., Barclay, L. D., Matyas, J. R., & Herzog, W. (2003). In situ chondrocyte deformation with physiological compression of the feline patellofemoral joint. *Journal of Biomechanics*, *36*(4), 553–568. https://doi.org/10.1016/S0021-9290(02)00424-4

Clark, A. L., Leonard, T. R., Barclay, L. D., Matyas, J. R., & Herzog, W. (2005). Opposing cartilages in the patellofemoral joint adapt differently to long-term cruciate deficiency: Chondrocyte deformation and reorientation with compression. *Osteoarthritis and Cartilage*, *13*(12), 1100–1114. https://doi.org/10.1016/j.joca.2005.07.010

Compton, D. R., Sheng, S., Carlson, K. E., Rebacz, N. A., Lee, I. Y., Katzenellenbogen, B. S., & Katzenellenbogen, J. A. (2004). Pyrazolo[1,5-α]pyrimidines: Estrogen receptor ligands possessing estrogen receptor β antagonist activity. *Journal of Medicinal Chemistry*, *47*(24), 5872–5893. https://doi.org/10.1021/jm049631k

Curtis, S. W., Washburn, T., Sewall, C., Diaugustine, R., Lindzey, J., Couse, J. F., & Korach, K. S. (1996). Physiological coupling of growth factor and steroid receptor signaling pathways: Estrogen receptor knockout mice lack estrogen-like response to epidermal growth factor. *Proceedings of the National Academy of Sciences of the United States of America*, *93*(22), 12626–12630. https://doi.org/10.1073/pnas.93.22.12626

Dantas, A. P. V., Franco, M. D. C. P., Silva-Antonialli, M. M., Tostes, R. C. A., Fortes, Z. B., Nigro, D., & Carvalho, M. H. C. (2004). Gender differences in superoxide generation in microvessels of hypertensive rats: Role of NAD(P)H-oxidase. *Cardiovascular Research*, *61*(1), 22–29. https://doi.org/10.1016/j.cardiores.2003.10.010

Dayani, N., Corvol, M.T., Robel, P., et al. (1988). Oestrogen receptors in cultured rabbit articular chondrocytes: influence of age. *J Steroid Biochem*. 31:351–6.

Ding, C., Cicuttini, F., Blizzard, L., Scott, F., Jones, G. (2006). A longitudinal study of the effect of sex and age on rate of change in knee cartilage volume in adults. *Rheumatol Adv Pract*. 46(2): 273-9.

Eckhoff, D. G. (2005). Functional Anatomy of the Knee. In J. Bellemans, M. D. Ries, & J. M. K. Victor (Eds.), *Total Knee Arthroplasty: A Guide to Get Better Performance* (pp. 18–24). https://doi.org/10.1007/3-540-27658-0_3

Eggli, P. S., Hunzinker, E. B., & Schenk, R. K. (1988). Quantitation of structural features characterizing weight- and less-weight-bearing regions in articular cartilage: A stereological analysis of medical femoral condyles in young adult rabbits. *The Anatomical Record*, *222*(3), 217–227. https://doi.org/10.1002/ar.1092220302

Elbaradie, K. B. Y., Wang, Y., Boyan, B. D., & Schwartz, Z. (2013). Sex-specific response of rat costochondral cartilage growth plate chondrocytes to 17β-estradiol involves differential regulation of plasma membrane associated estrogen receptors. *Biochimica et Biophysica Acta - Molecular Cell Research*, *1833*(5), 1165–1172. https://doi.org/10.1016/j.bbamcr.2012.12.022

Felson, D.T., Naimark, A., Anderson, J., Kazis, L., Castelli, W. and Meenan, R.F. (1987). The prevalence of knee osteoarthritis in the elderly: The Framingham Osteoarthritis Study. *Arthritis & Rheumatism*. **30**(8): 914-918.

Ffrench-Constant, C. (2003). Integrins. *Myelin Biology and Disorders*, *1*(Table 1), 609–632. https://doi.org/10.1016/B978-012439510-7/50078-4

Flandry, F., & Hommel, G. (2011). Normal anatomy and biomechanics of the knee. *Sports Medicine and Arthroscopy Review*, *19*(2), 82–92. https://doi.org/10.1097/JSA.0b013e318210c0aa

Fox, S. A. J., Bedi, A., & Rodeo, S. A. (2009). The basic science of articular cartilage: Structure, composition, and function. *Sports Health*, *1*(6), 461–468. https://doi.org/10.1177/1941738109350438

Fox, A. J. S., Bedi, A., & Rodeo, S. A. (2012). The Basic Science of Human Knee Menisci: Structure, Composition, and Function. *Sports Health*, *4*(4), 340–351. https://doi.org/10.1177/1941738111429419

Freed, D. M., Bessman, N. J., Kiyatkin, A., Salazar-Cavazos, E., Byrne, P. O., Moore, J. O., … Lemmon, M. A. (2017). EGFR Ligands Differentially Stabilize Receptor Dimers to Specify Signaling Kinetics. *Cell*, *171*(3), 683-695.e18. https://doi.org/10.1016/j.cell.2017.09.017

Freeman, P. M., Natarajan, R. N., Kimura, J. H., & Andriacchi, T. P. (1994). Chondrocyte cells respond mechanically to compressive loads. *Journal of Orthopaedic Research*, *12*(3), 311–320. https://doi.org/10.1002/jor.1100120303

Gardner, H., Kreidberg, J., Koteliansky, V., & Jaenisch, R. (1996). Deletion of integrin α1 by homologous recombination permits normal murine development but gives rise to a specific deficit in cell adhesion. *Developmental Biology*, *175*(2), 301–313. https://doi.org/10.1006/dbio.1996.0116

Girgert, R., Martin, M., Kruegel, J., Miosge, N., Temme, J., Eckes, B., … Gross, O. (2010). Integrin α2-deficient mice provide insights into specific functions of collagen receptors in the kidney. *Fibrogenesis & Tissue Repair*, *3*(1), 19. https://doi.org/10.1186/1755-1536-3-19

Glyn-Jones, S., Palmer, A.J.R., Agricola, R., Price, A.J., Vincent, T.L., Weinans, H., Carr, A.J. (2015). Osteoarthritis. *Lancet.* 386: 376-87.

Goldring, M. B. (2012). Chondrogenesis, chondrocyte differentiation, and articular cartilage metabolism in health and osteoarthritis. *Therapeutic Advances in Musculoskeletal Disease*, *4*(4), 269–285. https://doi.org/10.1177/1759720X12448454

Guilak, F., Erickson, G. R., & Ting-Beall, H. P. (2002). The effects of osmotic stress on the viscoelastic and physical properties of articular chondrocytes. *Biophysical Journal*, *82*(2), 720–727. https://doi.org/10.1016/S0006-3495(02)75434-9

Guilak, F., Ratcliffe, A., & Mow, V. C. (1995). Chondrocyte deformation and local tissue strain in articular cartilage: A confocal microscopy study. *Journal of Orthopaedic Research*, *13*(3), 410–421. https://doi.org/10.1002/jor.1100130315

Gupta, S., Hawker, G. A., Laporte, A., Croxford, R., & Coyte, P. C. (2005). The economic burden of disabling hip and knee osteoarthritis (OA) from the perspective of individuals living with this condition. *Rheumatology*, *44*(12), 1531–1537. https://doi.org/10.1093/rheumatology/kei049

Ha, K. Y., Chang, C. H., Kim, K. W., Kim, Y. S., Na, K. H., & Lee, J. S. (2005). Expression of estrogen receptor of the facet joints in degenerative spondylolisthesis. *Spine*, *30*(5), 562–566. https://doi.org/10.1097/01.brs.0000154674.16708.af

Hallbeck, A. L., Walz, T. M., Briheim, K., & Wasteson, Å. (2005). TGF-α and ErbB2 production in synovial joint tissue: Increased expression in arthritic joints. *Scandinavian Journal of Rheumatology*, *34*(3), 204–211. https://doi.org/10.1080/03009740510017715

Haskins, J. T. (2018). The sex-dependent interplay of integrin alpha1beta1 and epidermal growth factor receptor in regulating oxidative stress in articular cartilage. *The Atrium, University of Guelph.*

Hayashida, T., Jones, J. C. R., Lee, C. K., & Schnaper, H. W. (2010). Loss of β1-integrin enhances TGF-β1-induced collagen expression in epithelial cells via increased αvβ3-integrin and Rac1 activity. *Journal of Biological Chemistry*, *285*(40), 30741–30751. https://doi.org/10.1074/jbc.M110.105700

Henriksen, L., Grandal, M. V., Knudsen, S. L. J., van Deurs, B., & Grøvdal, L. M. (2013). Internalization Mechanisms of the Epidermal Growth Factor Receptor after Activation with Different Ligands. *PLoS ONE*, *8*(3). https://doi.org/10.1371/journal.pone.0058148

Hyder, S. M., Chiappetta, C., & Stancel, G. M. (1999). Interaction of human estrogen receptors α and β with the same naturally occurring estrogen response elements. *Biochemical Pharmacology*, *57*(6), 597–601. https://doi.org/10.1016/S0006-2952(98)00355-4

Hynes, R. O. (2002). Integrins: Bidirectional, Allosteric Signaling Machines. *Cell*, *110*, 673–687. https://doi.org/10.1016/B978-012439510-7/50078-4

Ide, T., Tsutsui, H., Ohashi, N., Hayashidani, S., Suematsu, N., Tsuchihashi, M., … Takeshita, A. (2002). Greater oxidative stress in healthy young men compared with premenopausal women. *Arteriosclerosis, Thrombosis, and Vascular Biology*, *22*(3), 438–442. https://doi.org/10.1161/hq0302.104515

Ignar-Trowbridge, D. M., Nelson, K. G., Bidwell, M. C., Curtis, S. W., Washburn, T. F., McLachlan, J. A., & Korach, K. S. (1992). Coupling of dual signaling pathways: Epidermal growth factor action involves the estrogen receptor. *Proceedings of the National Academy of Sciences of the United States of America*, *89*(10), 4658–4662. https://doi.org/10.1073/pnas.89.10.4658

Ingber, D. (1991). Integrins As Mechanochemical Transducers. *Current Opinion in Cell Biology*, *3*, 841–848.

Jablonski, C. L., Ferguson, S., Pozzi, A., & Clark, A. L. (2014). Integrin α1β1 participates in chondrocyte transduction of osmotic stress. *Biochemical and Biophysical Research Communications*, *445*(1), 184–190. https://doi.org/10.1016/j.bbrc.2014.01.157

Jeon, O. H., Campisi, J., Elisseeff, J. H., Jeon, O. H., David, N., Campisi, J., & Elisseeff, J. H. (2018). Senescent cells and osteoarthritis: a painful connection. *Journal of Clinical Investigation*, *128*(4), 1229–1237. https://doi.org/10.1172/JCI95147

Jia, H., Ma, X., Tong, W., Doyran, B., Sun, Z., Wang, L., … Qina, L. (2016). EGFR signaling is critical for maintaining the superficial layer of articular cartilage and preventing osteoarthritis initiation. *Proceedings of the National Academy of Sciences of the United States of America*, *113*(50), 14360–14365. https://doi.org/10.1073/pnas.1608938113

Jones, I. L., Klamfeldt, A., & Sandstrom, T. (1982). The effect of continuous mechanical pressure upon the turnover of articular cartilage proteoglycans in vitro. *Clinical Orthopaedics and Related Research*, *No. 165*, 283–289. https://doi.org/10.1097/00003086-198205000-00043

Kaab, M. J., AP Gwynn, I., & Notzli, H. P. (1998). Collagen fibre arrangement in the tibial plateau articular cartilage of man and other mammalian species. *Journal of Anatomy*, *193*(1), 23–34. https://doi.org/10.1046/j.1469-7580.1998.19310023.x

Kechagia, J. Z., Ivaska, J., & Roca-Cusachs, P. (2019). Integrins as biomechanical sensors of the microenvironment. *Nature Reviews Molecular Cell Biology*, *20*(8), 457–473. https://doi.org/10.1038/s41580-019-0134-2

Kim, Y. J., Sah, R. L. Y., Grodzinsky, A. J., Plaas, A. H. K., & Sandy, J. D. (1994). Mechanical regulation of cartilage biosynthetic behavior: Physical stimuli. *Archives of Biochemistry and Biophysics*, Vol. 311, pp. 1–12. https://doi.org/10.1006/abbi.1994.1201

King, L. K., March, L., & Anandacoomarasamy, A. (2013). Obesity & osteoarthritis. *Indian Journal of Medical Research*, *138*(AUG), 185–193.

Klinge, C. M. (2000). Estrogen receptor interaction with co-activators and co-repressors. *Steroids*, *65*(5), 227–251. https://doi.org/10.1016/S0039-128X(99)00107-5

Kumar, D., Souza, R.B., Subburaj, K., MacLeod, T.D., Singh, J., Calixto, N.E., Nardo, L., Link, T.M., Li, X., Lane, N.E., Majumdar, S. (2015) Are there sex differences in knee cartilage composition and walking mechanics in healthy and osteoarthritis populations? *Clin Orthop Relat Res.* 473: 2548-58.

Lees, D., & Partington, P. (2016). Articular cartilage. *Orthopaedics and Trauma*, *30*(3), 265–272. https://doi.org/10.1016/j.mporth.2016.04.007

Lepetsos, P., and Papavassiliou, A. G. (2016). ROS/oxidative stress signaling in osteoarthritis. Biochim. Biophys. Acta - Mol. Basis Dis. *1862*, 576–591.

Lindberg, K., Ström, A., Lock, J. G., Gustafsson, J. Å., Haldosén, L. A., & Helguero, L. A. (2010). Expression of estrogen receptor β increases integrin α1 and integrin β1 levels and enhances adhesion of breast cancer cells. *Journal of Cellular Physiology*, *222*(1), 156–167. https://doi.org/10.1002/jcp.21932

Loeser, R. F. (1997). Growth factor regulation of chondrocyte integrins: Differential effects of insulin-like growth factor 1 and transforming growth factor β on α1β1 integrin expression and chondrocyte adhesion to type VI collagen. *Arthritis and Rheumatism*, *40*(2), 270–276. https://doi.org/10.1002/art.1780400211

Loeser, R. F., Carlson, C. S., & McGee, M. P. (1995). Expression of β1 Integrins by Cultured Articular Chondrocytes and in Osteoarthritic Cartilage. *Experimental Cell Research*, Vol. 217, pp. 248–257. https://doi.org/10.1006/excr.1995.1084

Loeser, R. F., Sadiev, S., Tan, L., & Goldring, M. B. (2000). Integrin expression by primary and immortalized human chondrocytes: Evidence of a differential role for α1β1 and α2β1 integrins in mediating chondrocyte adhesion to types II and VI collagen. *Osteoarthritis and Cartilage*, *8*(2), 96–105. https://doi.org/10.1053/joca.1999.0277

Maroudas, A. (1980). Physical Chemistry of Articular Cartilage and the Intervertebral Disc. *The Joints and Synovial Fluid*, 239–291. https://doi.org/10.1016/B978-0-12-655102-0.50012-6

Maroudas, A., & Venn, M. (1977). Chemical composition and swelling of normal and osteoarthrotic femoral head cartilage. II. Swelling. *Annals of the Rheumatic Diseases*, *36*(5), 399–406. https://doi.org/10.1136/ard.36.5.399

Matthews, J., & Gustafsson, J. A. (2003). Estrogen signaling: a subtle balance between ER alpha and ER beta. *Molecular Interventions*, *3*(5), 281–292. https://doi.org/10.1124/mi.3.5.281

McGlashan, S. R., Jensen, C. G., & Poole, C. A. (2006). Localization of extracellular matrix receptors on the chondrocyte primary cilium. *Journal of Histochemistry and Cytochemistry*, *54*(9), 1005–1014. https://doi.org/10.1369/jhc.5A6866.2006

Migliaccio, A., Castoria, G., Di Domenico, M., Ciociola, A., Lombardi, M., De Falco, A., … Auricchio, F. (2006). Crosstalk between EGFR and extranuclear steroid receptors. *Annals of the New York Academy of Sciences*, *1089*, 194–200. https://doi.org/10.1196/annals.1386.006

Miller, T. T. (2009). Imaging of the medial and lateral ligaments of the knee. *Seminars in Musculoskeletal Radiology*, *13*(4), 340–352. https://doi.org/10.1055/s-0029-1242188

Nilsson, L. O., Boman, A., Savendahl, L., Grigelioniene, G., Ohlsson, C., Ritzen, E. M., & Wroblewski, J. (1999). Demonstration of Estrogen Receptor-Beta Immunoreactivity in Human Growth Plate Cartilage. *Journal of Clinical Endocrinology and Metabolism*, *84*(1), 370–373.

O'Hara, B. P., Urban, J., & Maroudas, A. (1990). Influence of cyclic loading on the nutrition of articular cartilage. *Annals of the Rheumatic Diseases*, *49*(7), 536–539. https://doi.org/10.1136/ard.49.7.536

Oshima, Y., Matsuda, K. I., Yoshida, A., Watanabe, N., Kawata, M., & Kubo, T. (2007). Localization of estrogen receptors α and β in the articular surface of the rat femur. *Acta Histochemica et Cytochemica*, *40*(1), 27–34. https://doi.org/10.1267/ahc.06015

Panday, A., Sahoo, M. K., Osorio, D., & Batra, S. (2015). NADPH oxidases: An overview from structure to innate immunity-associated pathologies. *Cellular and Molecular Immunology*, *12*(1), 5–23. https://doi.org/10.1038/cmi.2014.89

Parekh, R., Lorenzo, M. K., Shin, S. Y., Pozzi, A., & Clark, A. L. (2011). Integrin å1ß1 differentially regulates cytokine-mediated responses in chondrocytes. *Biological Bulletin*, *221*(1), 18–34. https://doi.org/10.1038/jid.2014.371

Pelletier, G. (2000). Localization of androgen and oestrogen receptors in rat and primate tissues. *Histol Histopathol*. 15:1261–1270.

Pest, M. A., Russell, B. A., Zhang, Y. W., Jeong, J. W., & Beier, F. (2014). Disturbed cartilage and joint homeostasis resulting from a loss of mitogen-inducible gene 6 in a mouse model of joint dysfunction. *Arthritis and Rheumatology*, *66*(10), 2816–2827. https://doi.org/10.1002/art.38758

Pettersson, K., & Gustafsson, J.-A. (2001). Role of Estrogen Receptor Beta in Estrogen Action. *Annu. Rev. Physiol.*, *63*, 165–192. https://doi.org/0066-4278/01/0315-0165

Poole, A. R. (1999). An introduction to the pathophysiology of osteoarthritis. *Frontiers in Bioscience: A Journal and Virtual Library*, *4*(6), 662–670. https://doi.org/10.2741/poole

Pujol, J. P., Chadjichristos, C., Legendre, F., Bauge, C., Beauchef, G., Andriamanalijaona, R., … Boumediene, K. (2008). Interleukin-1 and transforming growth factor-β 1 as crucial factors

in osteoarthritic cartilage metabolism. *Connective Tissue Research*, *49*(3–4), 293–297. https://doi.org/10.1080/03008200802148355

Puklin-Faucher, E., & Sheetz, M. P. (2009). The mechanical integrin cycle. *Journal of Cell Science*, *122*(4), 575. https://doi.org/10.1242/jcs.049544

Qin, L., & Beier, F. (2019). EGFR Signaling: Friend or Foe for Cartilage? *JBMR Plus*, *3*(2), e10177. https://doi.org/10.1002/jbm4.10177

Ramage, L. (2012). Integrins and Extracellular Matrix. *Cell Health and Cytoskeleton*, *4*, 1–9.

Ratcliff, A., Fryer, P. R., & Hardingham, T. E. (1984). The Distribution of Aggregating Proteoglycans in Articular Cartilage: Comparison of Quantitative Immunoelectron Microscopy with Radioimmunoassay and Biochemical Analysis. *The Journal of Histochemistry and Cytochemistry*, *32*(2), 193–201.

Rayego-Mateos, S., Rodrigues-Diez, R., Morgado-Pascual, J. L., Valentijn, F., Valdivielso, J. M., Goldschmeding, R., & Ruiz-Ortega, M. (2018). Role of epidermal growth factor receptor (EGFR) and its ligands in kidney inflammation and damage. *Mediators of Inflammation*, *2018*. https://doi.org/10.1155/2018/8739473

Rhee, D. K., Marcelino, J., Baker, M., Gong, Y., Smits, P., Lefebvre, V., … Carpten, J. D. (2005). The secreted glycoprotein lubricin protects cartilage surfaces and inhibits synovial cell overgrowth. *Journal of Clinical Investigation*, *115*(3), 622–631. https://doi.org/10.1172/JCI200522263.622

Richmond, R.S., Carlson, C.S., Register, T.C., Shanker, G., Loeser, R.F. (2000). Functional oestrogen receptors in adult articular cartilage: oestrogen replacement therapy increases chondrocyte synthesis of proteoglycans and insulin-like growth factor binding protein 2. *Arthritis Rheum*. 43:2081–90.

Roman-Blas, J. A., Castañeda, S., Largo, R., & Herrero-Beaumont, G. (2009). Osteoarthritis associated with estrogen deficiency. *Arthritis Research and Therapy*, *11*(5), 1–14. https://doi.org/10.1186/ar2791

Sah, R. L.-Y., Kim, Y.-J., Doong, J.-Y. H., Grodzinsky, A. J., Plaas, A. H. K., & Sandy, J. D. (2014). Biosynthetic response of cartilage explants to dynamic compression. *Classic Papers in Orthopaedics*, 427–429. https://doi.org/10.1007/978-1-4471-5451-8_108

Salkind, N. J. (2010). *Encyclopedia of Research Design*. SAGE Publications, Inc.

Salter, D. M., Hughes, D. E., Simpson, R., & Gardner, D. L. (1992). Integrin Expression By Human Articular Chondrocytes. *British Journal of Rheumatology*,*31*(4), 231-234. doi:10.1093/rheumatology/31.4.231

Schmidt, C., Pommerenke, H., Dürr, F., Nebe, B., & Rychly, J. (1998). Mechanical stressing of integrin receptors induces enhanced tyrosine phosphorylation of cytoskeletally anchored proteins. *Journal of Biological Chemistry*, *273*(9), 5081–5085. https://doi.org/10.1074/jbc.273.9.5081

Segal, A. W., & Abo, A. (1993). The biochemical basis of the NADPH oxidase of phagocytes. *Trends in Biochemical Sciences*, *18*(2), 43–47. https://doi.org/10.1016/0968-0004(93)90051-N

Selvakumar, B., Hess, D. T., Goldschmidt-Clermont, P. J., & Stamler, J. S. (2008). Co-regulation of constitutive nitric oxide synthases and NADPH oxidase by the small GTPase Rac. *FEBS Letters*, *582*(15), 2195–2202. https://doi.org/10.1016/j.febslet.2008.04.062

Sharif, B., Kopec, J., Bansback, N., Rahman, M. M., Flanagan, W. M., Wong, H., … Anis, A. (2015). Projecting the direct cost burden of osteoarthritis in Canada using a microsimulation model. *Osteoarthritis and Cartilage*, *23*(10), 1654–1663. https://doi.org/10.1016/j.joca.2015.05.029

Sharma, L., Chmiel, J.S., Almagor, O., Felson, D., Guermazi, A., Roemer, F., Lewis, C.E., Segal, N., Torner, J., Cooke, T.D., Hietpas, J., Lynch, J., Nevitt, M. (2013). The role of varus and valgus alignment in the initial development of knee cartilage damage by MRI: the MOST study. *Ann Rheum Dis.* 72: 235-40.

Sharma, L., Song, J., Felson, D. T., Cahue, S., Shamiyeh, E., & Dunlop, D. D. (2001). The role of knee alignment in disease progression and functional decline in knee osteoarthritis. *Journal of the American Medical Association*, *286*(2), 188–195. https://doi.org/10.1001/jama.286.2.188

Sharma, L., Song, J., Dunlop, D., Felson, D., Lewis, C.E., Segal, N., Torner, J., Cooke, T.D.V., Hietpas, J., Lynch, J., Nevitt, M. (2010). Varus and valgus alignment and incident and progressive knee osteoarthritis. *Ann Rheum Dis*. 69(11): 1940-5.

Shenoy, R., Pastides, P. S., & Nathwani, D. (2013). (iii) Biomechanics of the knee and TKR. *Orthopaedics and Trauma*, *27*(6), 364–371. https://doi.org/10.1016/j.mporth.2013.10.003

Shin, S. Y., Pozzi, A., Boyd, S. K., & Clark, A. L. (2016). Integrin α1β1 protects against signs of post-traumatic osteoarthritis in the female murine knee partially via regulation of epidermal growth factor receptor signalling. *Osteoarthritis and Cartilage*, *24*(10), 1795–1806. https://doi.org/10.1016/j.joca.2016.05.013

Sillem, M., Rabe, T., Prifti, S., Runnebaum, B., & Schmidt, M. (1997). Endometrial integrin expression is independent of estrogen or progestin treatment in vitro. *Fertility and Sterility*, *67*(5), 877–882. https://doi.org/10.1016/S0015-0282(97)81400-8

Sniekers, Y. H., van Osch, G. J. V. M., Ederveen, A. G. H., Inzunza, J., Gustafsson, J. Å., van Leeuwen, J. P. T. M., & Weinans, H. (2009). Development of osteoarthritic features in estrogen receptor knockout mice. *Osteoarthritis and Cartilage*, *17*(10), 1356–1361. https://doi.org/10.1016/j.joca.2009.04.008

Sniekers, Y. H., Weinans, H., Bierma-Zeinstra, S. M., van Leeuwen, J. P. T. M., & van Osch, G. J. V. M. (2008). Animal models for osteoarthritis: the effect of ovariectomy and estrogen treatment - a systematic approach. *Osteoarthritis and Cartilage*, *16*(5), 533–541. https://doi.org/10.1016/j.joca.2008.01.002

Tian, J., Zhang, F. J., & Lei, G. H. (2015). Role of integrins and their ligands in osteoarthritic cartilage. *Rheumatology International*, *35*(5), 787–798. https://doi.org/10.1007/s00296-014-3137-5

Touyz, R. M., & Schiffrin, E. L. (2004). Reactive oxygen species in vascular biology: Implications in hypertension. *Histochemistry and Cell Biology*, *122*(4), 339–352. https://doi.org/10.1007/s00418-004-0696-7

Umlauf, D., Frank, S., Pap, T., & Bertrand, J. (2010). Cartilage biology, pathology, and repair. *Cellular and Molecular Life Sciences*, *67*(24), 4197–4211. https://doi.org/10.1007/s00018-010-0498-0

Ushiyama, T., Ueyama, H., Inoue, K., Ohkubo, I., & Hukuda, S. (1999). Expression of genes for estrogen receptors α and β in human articular chondrocytes. *Osteoarthritis and Cartilage*, *7*(6), 560–566. https://doi.org/10.1053/joca.1999.0260

Valko, M., Leibfritz, D., Moncol, J., Cronin, M. T. D., Mazur, M., & Telser, J. (2007). Free radicals and antioxidants in normal physiological functions and human disease. *International Journal of Biochemistry and Cell Biology*, *39*(1), 44–84. https://doi.org/10.1016/j.biocel.2006.07.001

Van Beuningen, H. M., van der Kraan, P. M., Arntz, O. J., & van den Berg, W. B. (1994). Transforming growth factor-beta 1 stimulates articular chondrocyte proteoglycan synthesis and induces osteophyte formation in the murine knee joint. *Laboratory investigation; a journal of technical methods and pathology*, *71*(2), 279–290.

Van Beuningen, H. M., Glansbeek, H. L., Van Der Kraan, P. M., & Van Den Berg, W. B. (2000). Osteoarthritis-like changes in the murine knee joint resulting from intra-articular transforming growth factor-β injections. *Osteoarthritis and Cartilage*, *8*(1), 25–33. https://doi.org/10.1053/joca.1999.0267

Van der Eerden, B. C. J., Van Til, N. P., Brinkmann, A. O., Lowik, C. W. G. M., Wit, J. M., & Karperien, M. (2002). Gender differences in expression of androgen receptor in tibial growth plate and metaphyseal bone of the rat. *Bone*, *30*(6), 891–896. https://doi.org/10.1016/S8756-3282(02)00723-8

Vincent, T. L. (2013). Targeting mechanotransduction pathways in osteoarthritis: A focus on the pericellular matrix. *Current Opinion in Pharmacology*, *13*(3), 449–454. https://doi.org/10.1016/j.coph.2013.01.010

Wang, H., Chen, X., Su, Y., Paueksakon, P., Hu, W., Zhang, M. Z., … Pozzi, A. (2015). P47 phox contributes to albuminuria and kidney fibrosis in mice. *Kidney International*, *87*(5), 948–962. https://doi.org/10.1038/ki.2014.386

Wang, X., Fang, H., Huang, Z., Shang, W., Hou, T., Cheng, A., & Cheng, H. (2013). Imaging ROS signaling in cells and animals. *Journal of Molecular Medicine*, *91*(8), 917–927. https://doi.org/10.1007/s00109-013-1067-4

Wong, M., & Carter, D. R. (2003). Articular cartilage functional histomorphology and mechanobiology: A research perspective. *Bone*, *33*(1), 1–13. https://doi.org/10.1016/S8756-3282(03)00083-8

Woods, V. L., Schreck, P. J., Gesink, D. S., Pacheco, H. O., Amiel, D., Akeson, W. H., & Lotz, M. (1994). Integrin expression by human articular chondrocytes. *Arthritis & Rheumatism*, *37*(4), 537–544. https://doi.org/10.1002/art.1780370414

Wu, J. Z., & Herzog, W. (2000). Finite Element Simulation of Location- And Time-Dependent Mechanical Behavior of Chondrocytes in Unconfined Compression Tests. *Annals of Biomedical Engineering*, *28*(3), 318–330. https://doi.org/10.1114/1.271

Zemmyo, M., Meharra, E. J., Kühn, K., Creighton-Achermann, L., & Lotz, M. (2003). Accelerated, Aging-Dependent Development of Osteoarthritis in α1 Integrin-Deficient Mice. *Arthritis and Rheumatism*, *48*(10), 2873–2880. https://doi.org/10.1002/art.11246

Zhang, Y. W., Su, Y., Lanning, N., Swiatek, P. J., Bronson, R. T., Sigler, R., … Vande Woude, G. F. (2005). Targeted disruption of Mig-6 in the mouse genome leads to early onset degenerative joint disease. *Proceedings of the National Academy of Sciences of the United States of America*, *102*(33), 11740–11745. https://doi.org/10.1073/pnas.0505171102

Zhang, X., Zhu, J., Liu, F., Li, Y., Chandra, A., Levin, L. S., … Qin, L. (2014). Reduced EGFR signaling enhances cartilage destruction in a mouse osteoarthritis model. *Bone Research*, *2*(June). https://doi.org/10.1038/boneres.2014.15

Zhou, H.-B., Carlson, K. E., Stossi, F., Katzenellenbogen, B. S., & Katzenellenbogen, J. A. (2009). Analogs of Methyl-Piperidinopyrazole (MPP): Antiestrogens with Estrogen Receptor α Selective Activity. *Bioorg Med Chem Lett.*, *19*(1), 108–110. https://doi.org/10.1016/j.bmcl.2008.11.006

APPENDICES

Appendix A: Immunohistochemistry protocol for 3-nitrotyrosine

This protocol uses the Ultra-Sensitive ABC Peroxidase Staining Kit (Thermo Fisher), so the blocking solution, secondary antibody, and avidin-biotin complex (ABC) concentrations are calculated based on the kit's instructions.

Before starting, make sure to have designated waste bottles for 3% H_2O_2 in methanol, DAB, hematoxylin, ethanol, and xylene.

Materials:

- Cytoseal XYL (CAT#, Thermo Scientific)
- Fisherbrand Cover Slips 24mm X 60mm (12-545M, Fisher Scientific)
- Microscope slide box
- Slide holders (horizontally oriented)
- Kim wipes (82003-820, VWR)
- Squirt bottle
- Parafilm (52858-032, VWR)
- 100% Reagent Grade Ethanol (89370-084, VWR)
- 1xPBS diluted from 10xPBS (pH 7.4; 137mM sodium chloride, 2.7mM potassium chloride, 10mM sodium phosphate dibasic, 1.8mM potassium phosphate monobasic)
- Elite PAP pen (CA99990-104, VWR)
- 35% H_2O_2 (CAAAAL14000-AP, VWR)
- Methanol (CA71007-742, VWR)
- Ultra-Sensitive ABC Peroxidase Mouse IgG Staining Kit (32052, Thermo Fisher Scientific)
- SigmaFast 3,3'-Diaminobenzidine tablets (D4168-5SET, Sigma-Aldrich)
- Xylene (HC7001GAL, Thermo Fisher Scientific)
- Mouse monoclonal anti-nitrotyrosine primary antibody (ab61392, Abcam)
- Harris Modified Hematoxylin (SH26-500D, Fisher Scientific)
- Leica DM5000B Microscope (Leica Microsystems)

Steps:

DAY 1 (~ 2.5 - 3 hours)

1. Remove slides from the freezer and confirm the quality of the sections using a brightfield microscope. Assign the sections to a treatment group (blank (1 section), 2° only (1 section), and full (2 sections)).
2. Place slides in horizontally-oriented slide rack. Wash slides 3 x 5 min in 1xPBS (changing the PBS between each wash).
    - Each time you go in/out of a solution – dunk the rack 3-4 times, each time lifting it completely out of the liquid and letting it wash over the sections before submerging the rack again

- During the last wash step, prepare 3% H_2O_2 in methanol – mix 20 mL of 35% H_2O_2 in 180 mL of methanol
- **NOTE: this is a light-sensitive solution! Keep lights off in lab!**

3. To block endogenous peroxidases, place the slide rack in a slide holder with 3% H_2O_2 in methanol for 30 min (can cover slide holder with tin foil for extra light protection). At the end of the incubation, dump the 3% H_2O_2 in methanol into a designated waste container and rinse the slide holder.
4. Wash slides 3 x 5 min in 1xPBS.
    - While waiting for the washes, prepare blocking solution → 3.6% in 1xPBS – mix 1 drop of normal horse serum (~45 µL) in 1250 µL of 1xPBS
    - Also, prepare humidified chamber but placing paper towel at the bottom of an empty slide box and wetting the paper towel with water.
5. One at a time, take a slide out of 1xPBS, tap off and use a Kim wipe to blot excess liquid from the slides (careful not to touch the sections), then draw a circle around the sections using a hydrophobic PAP pen. DO NOT touch the sections or let them dry out!
    - Shake the PAP pen well before use!
    - DO NOT press too hard with the pen or it will explode all over the slide!
6. Lay slide in humidified chamber and apply 75 µL of blocking solution to every section.
7. Repeat steps 5 & 6 until all of the slides have blocking solution on the sections.
8. Incubate in the humidified chamber for ≥ 1 hour at room temperature.
9. Tilt slides lengthwise to allow for the blocking solution to run off the slides, tap off excess solution onto a paper towel and blot off any excess with a Kim wipe if necessary.
10. Place slides back into slide rack and wash slides 3 x 5 min in 1xPBS.
    - During the last wash step, prepare 1° antibody solution → anti-nitrotyrosine, 1:500 in blocking solution (4 slides worth → 1.24 µL of Ab in 618.76 µL of blocking solution)
    - Also, cut pieces of parafilm big enough to cover each section but not too big that they are overlapping with each other
11. One at a time, take a slide out of the 1xPBS solution, lay it flat in humidified chamber and place 75 µL of 1° antibody solution on the "full" sections. Place 75 µL of blocking solution on the "blank" and "2° only" sections. Repeat until all slides have solution on the sections. Gently place a piece of parafilm over each of the sections to help spread out the antibody solution over the section and to prevent the solution from completely evaporating (can use tweezers to help position the parafilm). Incubate overnight in the fridge at 4°C.
    - Put a sign on the fridge saying "Don't open the fridge, experiment in progress" to try to avoid the slides being ruined during overnight incubation

DAY 2 (~ 4 - 4.5 hours)

12. Remove the humidified slide box from the fridge and let it come to room temperature before opening the lid (~30 min).
13. Carefully remove the parafilm from each section using tweezers. One at a time, tilt slides lengthwise to allow for the antibody solution to run off the slides, tap off excess solution

onto a paper towel, and blot off any excess with a Kim wipe if necessary. Place into slide holder filled with 1xPBS. Repeat until all slides are in the slide rack.

- You want to make sure there is as little 1° antibody left on the sections as possible to avoid cross-contamination during the wash steps.

14. Wash slides 3 x 5 min in 1xPBS.
    - During the last wash step, prepare 2° antibody solution → approximately 1:222, made according to Kit directions (1 drop of antibody, 3 drops of NHS and 10 mL of 1 x PBS).
15. One at a time, take a slide out of the 1xPBS solution, lay it flat in humidified chamber and place 75 µL of 2° antibody solution onto "full" and "2° only" sections. Place 75 µL of blocking solution on "blank" section. Repeat until all slides have solution on the sections. Incubate for ≥ 1 hour at room temperature.
    - About halfway through incubation, prepare avidin-biotin complex (ABC) → to 2.5 mL of 1 x PBS, add 1 drop of Reagent A and 1 drop of Reagent B (from Ultra-Sensitive ABC Peroxidase Mouse IgG Staining Kit), mix and let sit for at least 30 min to properly conjugate.
16. One at a time, tilt slides lengthwise to allow for the antibody solution to run off the slides, tap off excess solution onto a paper towel, and blot off any excess with a Kim wipe if necessary. Place into slide holder filled with 1xPBS. Repeat until all slides are in the slide rack.
17. Wash slides 3 x 5 min in 1xPBS.
18. One at a time, take a slide out of the 1xPBS solution, lay it flat in humidified chamber and place 75 µL of ABC on "full" and "2° only" sections. Place 75 µL of blocking solution on "blank" section. Repeat until all of the slides have solution on the sections. Incubate for 30 min at room temperature.
19. One at a time, tilt slides lengthwise to allow for the ABC solution to run off the slides, tap off excess solution onto a paper towel, and blot off any excess with a Kim wipe if necessary. Place into slide holder filled with 1xPBS. Repeat until all slides are in the slide rack.
20. Wash slides 3 x 5 min in 1xPBS.
    - During the last wash step, prepare the DAB solution from the Sigma Fast 3,3'-diaminobenzidine tablets → place one silver and one gold tablet in 1 mL of MilliQ water and invert to mix (makes enough solution for 4 slides).
21. One at a time, take a slide out of 1xPBS, lay it flat in humidified chamber and place 62.5 µL of DAB solution on every section. Repeat until all of the slides have solution on the sections. Place DAB-contaminated pipette tips in biohazard dry waste bin. Incubate for 15 min at room temperature.
    - NOTE: This step is very time sensitive. Start the 15 min timer after solution has been put on the first slide and rinse the slides in the same order that you apply the solution to account for the difference in application time.
22. One at a time, tilt the slides lengthwise and tap off DAB solution <u>into a beaker</u> then use a squirt bottle filled with MilliQ water to gently squirt water on the top edge of the slide, allowing the water to wash over the sections and catching the waste in the beaker (DO NOT squirt water directly onto the sections). Place rinsed slides back into slide rack and

into a slide holder of MilliQ water. Repeat until all of the slides have been rinsed. Dispose of liquid DAB waste in a designated waste container.

23. Dunk slides 4-5 times in MilliQ water then wash 2 x 5 min.
    - During the wash steps, prepare the washes for after the counterstain step → two large beakers of deionized water and 3 slide holders of MilliQ water
24. To counterstain, place up to 4 slides at a time in a vertically-oriented rack in hematoxylin for 10 seconds. Rinse slides in the two beakers of deionized water (~4-5 dunks in each) before transferring slides back into horizontally-oriented rack, and dunk ~4-5 times in MilliQ water and then wash 2 x 5 min in fresh MilliQ water.
25. Transfer slides through a series of 5 min soaks in 70%, 95%, and 100% ethanol. Dispose of ethanols in designated liquid waste container.
26. Soak slides in xylene for 5 min. Dispose of xylene in designated waste container.
27. Apply a thin strip of Cytoseal XYL along the long edge of the slide and coverslip by pushing a 'wave' of Cytoseal from one side of the slide to the other. After allowing the Cytoseal to set for ~1-2 min, firmly press on each section with your thumb or forefinger. Change gloves if they become sticky. Let slides dry for about 10 min before moving and let Cytoseal cure overnight at room temperature.
28. The next day, if there is any excess Cytoseal dried on the surface of the slide, use a razor blade to carefully scrape it off.
29. Image sections using a bright-field microscope (Leica DM5000B microscope).

Appendix B: Immunofluorescence Protocol for ERα and ERβ

Materials:

- Microscope slide box
- Slide holders (horizontally oriented)
- Kim wipes (82003-820, VWR)
- Squirt bottle (76263-148, VWR)
- Parafilm (52858-032, VWR)
- 1xPBS diluted from 10xPBS with MilliQ water (10xPBS → pH 7.4; 137mM sodium chloride, 2.7mM potassium chloride, 10mM sodium phosphate dibasic, 1.8mM potassium phosphate monobasic)
- Elite PAP pen (CA99990-104, VWR)
- Normal Goat Serum (10000C, Life Technologies)
- Mouse monoclonal anti-ERα [1D5] (MA5-13191, Thermo Fisher Scientific)
- Rabbit polyclonal IgG anti-ERβ (PA1-310B, Thermo Fisher Scientific)
- Goat anti-mouse IgG (H+L) $F(ab')_2$ fragment Alexa Fluor 647 (A21237, Thermo Fisher Scientific)
- Goat anti-rabbit IgG (H+L) Alexa Fluor 555 (A21428, Thermo Fisher Scientific)
- Hoechst 33342 (H1399, Invitrogen)
    - Stock Solution (16.23 mM) → 10mg of powder in 1mL of MilliQ water
    - Working Solution (0.1mM) → 30.56 μL of stock in 4929.44 μL of Milli Q water (makes enough for 8 aliquots of 620 μL → 16 slides)
- Prolong Gold (P36930, Thermo Fischer Scientific)
- Fisherbrand Cover Slips 24mm X 60mm (12-545M, Fisher Scientific)
- Nail polish (any brand/colour)

Steps:

DAY 1 (~2 hours)

1. Remove slides from the freezer and confirm the quality of the sections using a brightfield microscope. Assign the sections to a treatment group (blank (1 section), 2° only (1 section), and full (2 sections)). Allow slides to come to room temperature before beginning (~10-15 min).
2. Place slides in horizontally-oriented slide rack. Wash slides 3 x 5 min in 1xPBS (changing the PBS between each wash).
    - Each time you go in/out of a solution – dunk the rack 3-4 times, each time lifting it completely out of the liquid and letting it wash over the sections before submerging the rack again
    - During the wash steps, prepare the blocking solution → 5% normal goat serum in 1xPBS (300 μL NGS in 5700 μL of 1xPBS)
        - This is enough blocking solution for the whole run (4 slides) + extra
        - Can be stored in the fridge and used as needed for the blocking steps, to put on the blank sections during incubation periods, and to dilute the antibodies

- Also, prepare humidified chamber but placing paper towel at the bottom of an empty slide box and saturating the paper towel with tap water.

3. One at a time, take a slide out of 1xPBS, tap off excess solution onto a paper towel and blot off any excess with a Kim wipe if necessary (careful not to touch the sections), then draw a circle around the sections using a hydrophobic PAP pen. DO NOT touch the sections or let them dry out!
    - Shake the PAP pen well before use!
    - DO NOT press too hard with the pen or it will explode all over the slide!
    - Can test PAP pen on blank slide to make sure that it is working properly
4. Lay slide in humidified chamber and apply 75 μL of blocking solution to every section.
    - Make sure that the tissue sections are completely covered by blocking solution.
5. Repeat steps 3 & 4 until all of the slides have blocking solution on the sections.
6. Incubate in the humidified chamber for ≥ 1 hour at room temperature.
7. One at a time, tilt slides lengthwise (horizontally) to allow for the blocking solution to run off the slides, tap off excess solution onto a paper towel and blot off any excess with a Kim wipe if necessary. Place slide in slide holder filled with 1xPBS before moving on to the next slide to prevent the sections from drying out. Repeat until all the slides are in the slide holder.
8. Wash slides 3 x 5 min in 1xPBS.
    - During the last wash step, prepare 1° antibody solution → anti-ERα and anti-ERβ both at 1:200) – for each Ab, mix 3.1 μL of Ab in 306.9 μL of blocking solution and then mix the two antibody solutions together
        - This is enough for 4 slides (2 sections per slide)
    - Cut pieces of parafilm big enough to cover each section but not too big that they are overlapping with each other
9. One at a time, take a slide out of the 1xPBS solution, lay it flat in humidified chamber and place 75 μL of 1° antibody solution on the "full" sections. Place 75 μL of blocking solution on the "blank" and "2° only" sections. Repeat until all slides have solution on the sections. Gently place a piece of parafilm over each of the sections to help spread out the antibody solution over the section and to prevent the solution from completely evaporating (can use tweezers to help position the parafilm). Incubate overnight in the fridge at 4°C.
    - Put a sign on the fridge saying "Don't open the fridge, experiment in progress" to try to avoid the slides being ruined during overnight incubation

DAY 2 (~3 hours)

10. Remove the humidified slide box from the fridge and let it come to room temperature before opening the lid (~30 min).
11. Carefully remove the parafilm from each section using tweezers. One at a time, tilt the slides lengthwise (horizontally) to allow for the antibody solution to run off the slides, tap off excess solution onto a paper towel, and blot off any excess with a Kim wipe if necessary. Place slide in slide holder filled with 1xPBS before moving on to the next slide to prevent the sections from drying out. Repeat until all the slides are in the slide holder.

- You want to make sure there is as little 1° antibody left on the sections as possible to avoid cross-contamination during the wash steps.

12. Wash slides 3 x 5 min in 1xPBS.
    - During the last wash step, prepare 2° antibody solution → F(ab') AF647 for ERα and AF555 for ERβ both at 1:500 – for each Ab, mix 1.84 µL of Ab in 458.16 µL of blocking solution then mix the two antibody solutions together
        - This is enough for 4 slides (3 sections per slide)
    - **NOTE: Samples are light-sensitive beyond this point → Keep lab lights off during remainder of experiment!!**
13. One at a time, take a slide out of the 1xPBS solution, lay it flat in humidified chamber and place 75 µL of 2° antibody solution onto "full" and "2° only" sections. Place 75 µL of blocking solution on "blank" section. Make sure that all tissue sections are completely covered by the solution. Repeat until all slides have solution on the sections. Incubate for ≥ 1 hour at room temperature.
14. One at a time, tilt slides lengthwise to allow for the antibody solution to run off the slides and tap off excess solution on a paper towel. Use a squirt bottle filled with 1xPBS to gently squirt along the top edge of the slide, allowing the PBS to wash over the sections and catching the waste in a beaker (DO NOT squirt directly onto the sections to avoid damaging the tissue sections or completely washing them off the slide). Place slide in slide holder filled with 1xPBS before moving on to the next slide to prevent the sections from drying out. Repeat until all the slides are in the slide holder.
    - What is collected in the beaker can be disposed of down the sink
15. Wash slides 3 x 5 min in 1xPBS.
    - During first wash step, remove 0.1M Hoechst working solution from the freezer to thaw completely before use
16. One at a time, take a slide out of the 1xPBS solution, lay it flat in humidified chamber and place 75 µL of Hoechst on all sections. Make sure that all tissue sections are completely covered by the solution. Repeat until all slides have solution on the sections. Incubate for 5 min at room temperature.
17. One at a time, tilt the slides lengthwise (horizontally) and tap off Hoechst solution into a beaker then use a squirt bottle filled with MilliQ water to gently squirt water along the top edge of the slide, allowing the water to wash over the sections and catching the waste in the beaker (DO NOT squirt water directly onto the sections). Place rinsed slide into horizontal slide rack and submerge in MilliQ water before moving onto the next slide. Repeat until all of the slides have been rinsed. Dispose of Hoechst waste in a designated waste container.
18. Dunk slides 4-5 times in MilliQ water then wash 2 x 5 min (changing the water between each wash).
19. Carefully dry excess water off slides using a Kim wipe (DO NOT touch the tissue section). Pipette a thin strip of Prolong Gold along the long edge of the slide (~100 µL) and coverslip by pushing a 'wave' of Prolong Gold from one side of the slide to the other. After allowing the slide to set for ~1-2 min, firmly press on each section with your thumb or forefinger. Change gloves if they become sticky. Let slides dry for about 10 min before moving and let slides cure overnight at room temperature in a dark place (i.e. inside a slide box).

DAY 3

20. After curing and before imaging, paint around the edges of the coverslip with nail polish to help seal the edges and prevent the coverslip from moving.